Volume 10, no. 1, January-April 2021

ISSN 2038-4106/2021 (print)

European Journal of Musculoskeletal Diseases

Sebastiano del Piombo, *Resurrezione di Lazzaro*, olio su tela, 1516-1519, National Gallery, London *(detail)*.

Published by
Biolife

www.biolife-publisher.it

European Journal of Musculoskeletal Diseases
ISSN 2038-4106/2021

BPI

Eur J Musculoskel Dis 2021 Jan-Apr issue 1

CONTENTS

European Journal of Musculoskeletal Diseases
ISSN 2038-4106/2021

Comparative Study

MODIFIED ORALHYGIENE PROTOCOLS TO PREVENT PERIODONTAL DISEASES. ROLE OF LASERS AND PHASE CONTRAST MICROSCOPES IN PERIODONTAL MAINTENANCE THERAPY

G. Caccianiga[1], P. Erba[2], G. Caccianiga[2] and P. Caccianiga[1*]

[1]School of Medicine and Surgery, University of Milano-Bicocca, Monza, Italy;
[2]Private Practicioner, Bergamo, Italy

**Correspondence to:*
Paolo Caccianiga, DDS
School of Medicine and Surgery, University of Milano-Bicocca, 20900 Monza, Italy
e-mail: p.caccianiga@campus.unimib.it

ABSTRACT

The purpose of this research was to assess how the application of the oral irrigator modifies the bacterial flora using a phase contrast microscope in patients affected by chronic periodontitis and treated with laser and strictly home care protocol.

60 patients were included in periodontal maintenance therapy (PMT), with specific home oral hygiene instructions (sonic toothbrush plus oral irrigators, at least twice a day). Phase contrast-phase microscopic examinations displayed the existence of non-mobile (i.e., not pathologic) bacterial flora in all patients. They were then randomly divided into two groups, A and B. After professional oral hygiene, group A stops using an oral irrigator at home. After the professional oral hygiene, patients of group B were motivated to continue their oral hygiene protocol at home. After three months, the patients underwent a second microscopic analysis of bacterial plaque.

In the Group A patients, 90% of cases had a pathogenic bacterial flora change. 100% of the patients in group B showed non-mobile bacteria on phase contrast microscopic analysis, whereas group A showed mobile bacteria.

This research demonstrates that oral irrigator in home hygiene protocol plays a role in the long-term maintenance of non-pathogenic bacterial flora in periodontal patients.

KEYWORDS: *bacterial flora, oral irrigator, diode laser, hydrogen peroxide, oral hygiene, oral irrigator, phase contrast microscopy, photodynamic therapy, sonic toothbrush.*

INTRODUCTION

Maintaining periodontal health over time is crucial in guaranteeing the success of dental treatments. Periodontal maintenance therapy (PMT) and home oral hygiene protocols are the keys to success. We know from the literature and clinical experiences that without meticulously organized and performed PMT, patients with a predisposition to periodontal disease are at high risk of reinfection and progression of periodontal lesions. A large amount of failures after non-surgical

Received: 22 October 2020
Accepted: 05 January, 2021

ISSN: 2038-4106

or surgical periodontal therapies (1) is due to incomplete cleaning of the root superficies from bacteria belonging to red and orange Socransky's complexes, such as *Porphyromonas gingivalis*, *Treponema denticola*, *Bacteroides forsythus*, *Fusobacterium nucleatum,* and *Peptostreptococcus micros*. It has been shown (2) that new contamination of the periodontal pockets is total after a one-year follow-up, even with frequent dentist appointments, either with non-surgical or surgical therapies.

Since the 90s, reports have shown that decontamination by laser radiation is possible (3). Lasers can be applied alone or in association with a photosensitizer. Photodynamic therapy (PDT) is the association of light with a chromophore and oxygenated tissues (4). This technique aims to bring singlet oxygen to all tissues affected by pathogenic bacteria. However, if chromophores absorb the wavelengths, laser rays cannot break through tissues very deep. In addition, if the power density is too low, the decontaminating effects are insufficient. It happens because PDT protocols use LLLT (low-level laser therapy) energy to avoid thermal damage.

Recent research (5) proposed a combination between high power and high frequency of diode laser 980 nm (using high peak power combined with low average power to reduce thermal effects) and hydrogen peroxide 10 volume 3%, or modified hydrogen peroxide 10 volumes 3%. This treatment protocol has been named "photodynamic therapy without dye" or Oxygen High Level Laser Therapy (6). Several in vitro and in vivo studies showed the bactericidal activity of laser irradiation combined with hydrogen peroxide (7).

The aim of this research was to evaluate how much homecare with an oral irrigator has a role in maintaining a non-pathogenic bacterial flora in the oral cavity. The diagnostic tool is the phase contrast microscope (8) which provides qualitative data on the bacterial flora monitored during the six-monthly recalls of professional hygiene.

MATERIALS AND METHODS

The present study was carried out in conformity with the Declaration of Helsinki. Sixty patients from a private dental clinic in Bergamo, Italy, were recruited and were diagnosticated moderate generalized periodontitis in 2016, 2017, and 2018. In addition, they had laser-assisted non-surgical therapy and taught in-homecare protocol with a sonic toothbrush, interdental brush and oral irrigator. Subsequently, they underwent a second clinical evaluation in order to be sure that periodontal disease was stabilized. Afterwards, they were recruited in a 6-months recall protocol of professional oral hygiene.

For the periodontal maintenance therapy, the following maintenance home hygiene protocol was delivered: sonic brush with vertical movement (Broxo OraBrush, Santé Parodonte, Geneva, Switzerland), interdental brushes, and oral irrigators (Broxo OraJets, Santé Parodonte, Geneva, Switzerland) at least two times every day (Fig. 1-2-3).

Fig. 1. *Oral hygiene devices. Seven devices for optimal domiciliary hygiene procedures. The most important are: 1: manual toothbrush; 1: sonic brush with vertical movement; 2: interdental brushes; 3: oral irrigators.*

An evaluation of the subgingival plaque sample was performed on each patient by using contrast-phase microscopy. It was performed during PMT appointments every 6 months in a close recall scheme (Fig. 4-5).

Based on contrast phase microscopy results, two protocols were applied. In the case of non-pathogenic bacterial flora (i.e. static flora, Gram-positive bacteria) detection, standard periodontal therapy with appointments every 6 months was delivered. In the case of pathogenic bacterial flora (spirochete, moving flora) detection, immediate treatment with supra-gingival and sub-gingival ultrasonic instrumentation, air flow with bicarbonate powder, and a single-session of photodynamic therapy without dye (OHLLT) in the entire mouth was delivered. The last protocol has also been applied without signs of inflammation (i.e. pain, bleeding).

The single-stage session of photodynamic therapy without dye (OHLLT) is the irrigation of periodontal pockets with a Sioxyl solution. First, the operator aspires a Sioxyl solution from the gingival sulcus, leaving the remaining solution inside the pocket for 2 min. After that, an HF Diode Laser 980 nm, Fiber 400 microns (Wiser Doctor Smile, Lambda, Vicenza, Italy) is introduced in the periodontal pocket to reach the bottom. Then, radiation of subgingival tissues is carried out through a back-and-forth movement, using a specific program, 60 s for each side (2.5 W peak power, high frequency, 10 kHz, power average 0.5 W, Fluency 25000/cm2).

At the end of the professional oral hygiene procedure, patients were trained for homecare protocol with a sonic brush, interdental brushes, and oral irrigator at least twice daily.

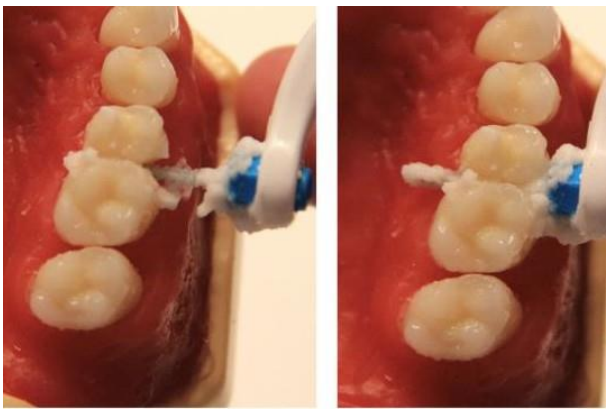

Fig. 2. *Interdental brushes.*

Fig. 3. *Oral irrigator during subgingival biofilm removal.*

After 1 month, patients were checked for periodontal disease with a contrast-phase microscope. If they have only non-pathogenic bacterial flora, patients returned to standard 6-month controls. If they have pathogenic bacterial flora, patients are trained again for oral hygiene associated with a single-stage session of laser-assisted PDT without dye.

Dental hygienists, therefore, are responsible for organizing this specific prevention and maintenance program, personalized and flexible, using a continuous and progressive educational process that can support the results obtained by the dentist.

All 60 patients recruited in periodontal support therapy had the following inclusion criteria:

- age from 35 to 65;
- no systemic diseases;
- periodontal clinical attachment loss of less than 5mm in at least two teeth;
- no tooth mobility;
- bleeding index under 30%;
- plaque index under 30%.

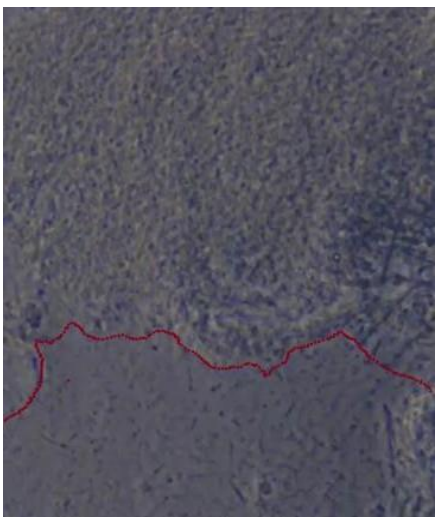

Fig. 4. *Contrast phase microscope with dividing line between non-pathogenic bacterial flora (above) and pathogenic bacterial flora (below).*

All 60 patients were evaluated for subgingival plaque check with a phase contrast microscope by the same operator. For examination, a periodontal curette is used. It collected bacterial plaque in the gingival sulcus. First, plaque is placed on a slide, then it is irrigated with a drop of physiological solution, fixed with a counterslide, and a drop of oil is placed on the counterslide to concentrate the light of the microscope. A 40x objective is recommended with an eyepiece of 15x (600 magnification).

Then it is possible to visualize which kind of bacteria are present in the plaque, as well as epithelial cells and polymorphonuclear cells. Contrast-phase microscope distinguishes between a non-pathogenic bacterial flora (Fig. 6) that is non-mobile and a pathogenic bacterial flora (Fig. 7) that is primarily mobile and composed of spirochetes such as Treponema Denticola.

The plaque was collected from the gingival sulcus in each patient. Microscopic analysis showed non-pathogenic bacterial flora for each sample (T0). All patients were then randomly divided into two groups, A and B. After a professional oral hygiene session, group A was asked to suspend the use of an oral irrigator and continue the home hygiene protocol only with a sonic toothbrush and interdental brushes. After the professional oral hygiene session, Group B was requested to continue the complete homecare protocol. Three months later, the patients underwent a second bacterial plaque analysis (T1), and the data were obtained and accessed through the Statistical Package for Social Sciences (SPSS).

Fig. 5. *Contrast-phase microscope.*

RESULTS

Patients belonging to Group A (Table I) (i.e. did not use the oral irrigator) had mobile bacterial flora in 90% of cases. Instead, 100% of patients belonging to group B (i.e. using the standard protocol with a sonic toothbrush, interdental brushes and oral irrigator for 3 months) showed non-mobile plaque on phase contrast microscopic evaluation.

Recruited patients had a plaque index of less than 30% (Table II). At the time of re-evaluation, group A showed a slight worsening of the plaque index: seven out of 30 patients had a plaque index greater than 30%. In group B, there was no worsening of the plaque index. The control group maintained the plaque index below 30% in all cases.

Table III and Table IV report the difference between periodontal and microbial parameters of groups A and B at T0 and T1, demonstrating that oral irrigator usage at home effectively maintains a non-mobile flora in the periodontal sulcus.

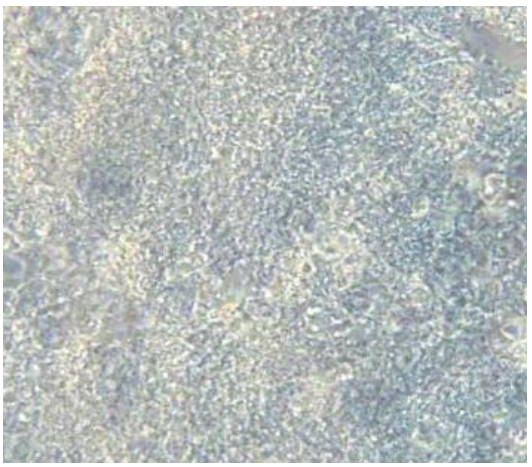

Fig. 6. *Non-pathogenic bacterial flora.*

DISCUSSION

The phase contrast microscope uses two principles (wavelength and amplitude) to create an image of cells (8, 9). Methodologically, contamination, sampling technique and sample preparation are important as they strongly influence the analysis result. The reproducibility of what is seen using contrast phase microscopy is high when the procedure is standardized. Sample analysis gives us some clinically relevant information (8, 10). Direct examination of the sub-gingival dental plaque under a phase contrast microscope allows one to characterize bacterial morphotypes without inflammatory signs. It also allows for evaluating the microbial density associated, or not, with active periodontal pockets.

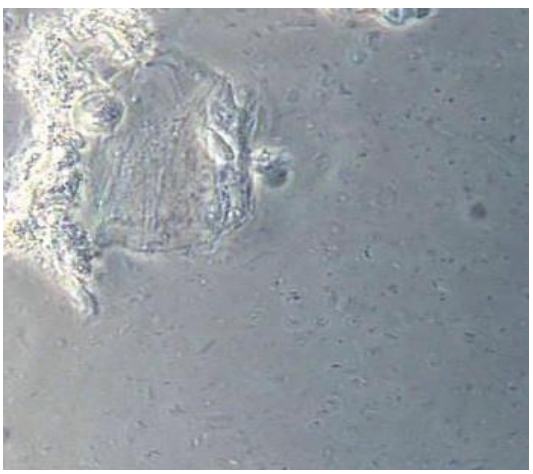

Fig. 7. *Pathogenic bacterial flora.*

Phase contrast microscopy provides qualitative data of bacterial flora that integrates the standard periodontal parameters such as plaque index, bleeding index and loss of clinical attachment collected and monitored during the six-monthly recalls of professional hygiene. Quirynen et al. (11) based the results of their research on the phase contrast microscope. Bollen, et al.,

(12) published a pilot study examining the long-term microbiological effects of a "full mouth" disinfection controlled with phase contrast microscopy. Yeom et al. (13) used the phase contrast microscope to evaluate the clinical and microbiological effects of the subgingival deposition of bioabsorbable microcapsules loaded with 10% of minocycline in 15 adult patients with periodontitis. Quirynen et al. (14) used a phase contrast microscope to evaluate the bacterial plaque around the implant surfaces. Acharya et al. (15) compared the efficacy of three motivational techniques to maintain good oral hygiene during fixed appliance orthodontic treatment. Phase contrast microscopy and the conventional plaque detection method were used to demonstrate that vertical brushing is the best; this reduces the need for frequent strengthening sessions of plaque control programs.

Analysis of the literature demonstrated that homecare periodontal support therapy could preferably include a sonic electric toothbrush (16-18) for the shock wave generated by the movement of the bristles combined with the oral irrigator (19-21). This last induces the solution of subgingival plaque through the disorganization of the salivary biofilm, which can potentially spread microorganisms in the gingival sulcus (1, 2, 22).

The present study demonstrated that using a specific home oral hygiene protocol is essential in periodontal maintenance therapy. Oral irrigators are important to maintain a non-pathogenic bacterial flora in subgingival plaque. If patients in

Table I. *Patients with not-mobile flora at first (T0) and second (T1) evaluation.*

Compatible flora	T_0	T_1
Group A	30	3
Group B	30	30

Table II. *Patients with plaque index less than 30% at first (**T0**) and second evaluation (**T1**).*

Plaque index < 30%	T_0	T_1
Group A	30	23
Group B	30	30

Table III. *Periodontal and microbial parameters among the A group and B group at T0.*

	Group A (n = 30)	Group B (n = 30)	p Value
	Mean ± sd	**Mean ± sd**	
BoP	0.14 ± 0.09	0.11 ± 0.10	<0.018
P.I.	0.23 ± 0.12	0.21 ± 0.11	0.006
P. D.	2.24 ± 0.23	2.25 ± 0.21	0.267

***BoP**: bleeding on probing; **P.I.**: plaque index; and **P.D.**: periodontal depth. *p value <0.001 is statistically significant.*

Table IV. *Periodontal and microbial parameters among the A group and B group at T1.*

	Group A (n = 30)	Group B (n = 30)	p Value
	Mean ± sd	**Mean ± sd**	
BoP	0.12 ± 0.05	1.12 ± 0.21	<0.0005 *
P.I.	0.12 ± 0.15	0.93 ± 0.21	<0.001 *
P.D.	2.16 ± 0.18	2.41 ± 0.24	0.135

***BoP**: bleeding on probing; **P.I.**: plaque index; and **P.D.**: periodontal depth. *p value <0.001 is statistically significant.*

PMT avoid using oral irrigators for 3 months, periodontal conditions deteriorate with an increase of pathogenic bacterial flora detected with phase contrast microscopy and worst periodontal parameters (PI, BOP, PD).
The patient must be constantly monitored and continuously remotivated to maintain excellent oral hygiene levels. Scientific literature proves that our protocol is a suitable method to stop the onset and advancement of periodontal infection. It also avoids relapses and stabilizes the results obtained in patients predisposed to periodontal disease.

CONCLUSION

The present study shows that phase contrast microscopy detects early sub-gingival plaque modifications due to poor home oral hygiene protocols application by patients and how the use of the oral irrigator is of paramount importance in the long-term maintenance of a non-pathogenic bacterial flora in the periodontal sulcus. It is clear that, although it is possible to maintain an acceptable plaque index only with a sonic toothbrush and pipe cleaners, a water jet allows the maintenance of non-pathogenic bacterial flora in the oral cavity of patients who have not stopped using it.

Institutional Review Board Statement

The study was conducted according to the guidelines of the Declaration of Helsinki. Informed consent was obtained from all subjects involved in the study.

Author Contributions

GLC and PC designed the research study; PE and GC performed the research; GLC and PC wrote the manuscript. All authors contributed to editorial changes in the manuscript and read and approved the final version. The authors declare no conflict of interest.

REFERENCES

1. Rhemrev GE, Timmerman MF, Veldkamp I, Van Winkelhoff AJ, Van der Velden U. Immediate effect of instrumentation on the subgingival microflora in deep inflamed pockets under strict plaque control. *Journal of Clinical Periodontology*. 2006;33(1):42-48. doi:10.1111/j.1600-051X.2005.00871.x
2. Heitz-Mayfield L, Tonetti MS, Cortellini P, Lang NP, European Research Group on Periodontology (ERGOPERIO). Microbial colonization patterns predict the outcomes of surgical treatment of intrabony defects. *Journal of Clinical Periodontology*. 2006;33(1):62-68. doi:10.1111/j.1600-051X.2005.00872.x
3. Gursoy H, Ozcakir-Tomruk C, Tanalp J, Yılmaz S. Photodynamic therapy in dentistry: a literature review. *Clinical Oral Investigations*. 2013;17(4):1113-1125. doi:10.1007/s00784-012-0845-7
4. Azarpazhooh A, Shah PS, Tenenbaum HC, Goldberg MB. The Effect of Photodynamic Therapy for Periodontitis: A Systematic Review and Meta-Analysis. *Journal of Periodontology*. 2010;81(1):4-14. doi:10.1902/jop.2009.090285
5. Caccianiga G, Rey G, Baldoni M, Paiusco A. Clinical, Radiographic and Microbiological Evaluation of High Level Laser Therapy, a New Photodynamic Therapy Protocol, in Peri-Implantitis Treatment; a Pilot Experience. *BioMed Research International*. 2016;2016:6321906. doi:10.1155/2016/6321906
6. Rey G. L'apport du laser dans le traitement des poches paradontales. *Implantodontie*. 2000;38:37-44.
7. Caccianiga G, Baldoni M, Ghisalberti CA, Paiusco A. A Preliminary In Vitro Study on the Efficacy of High-Power Photodynamic Therapy (HLLT): Comparison between Pulsed Diode Lasers and Superpulsed Diode Lasers and Impact of Hydrogen Peroxide with Controlled Stabilization. *BioMed Research International*. 2016;2016:1386158. doi:10.1155/2016/1386158
8. Callens A. [Darkfield or phase contrast microscopy. Usefulness in periodontology]. *Nederlands Tijdschrift Voor Tandheelkunde*. 1992;99(10):381-384.
9. Rose GG. Phase-contrast microscopy in living cells. *Journal of the Royal Microscopical Society*. 1964;83(1-2):97-114. doi:10.1111/j.1365-2818.1964.tb00517.x
10. Leggott PJ, Anderson AW, Punwani I, Sabet T, Murphy R, Crawford J. Phase contrast microscopy of microbial aggregates in the gingival sulcus of Macaca mulatta. Subgingival plaque bacteria in macaca mulatta. *Journal of Clinical Periodontology*.

1983;10(4):412-421. doi:10.1111/j.1600-051x.1983.tb01290.x

11. Quirynen M, Mongardini C, de Soete M, et al. The role of chlorhexidine in the one-stage full-mouth disinfection treatment of patients with advanced adult periodontitis. Long-term clinical and microbiological observations. *Journal of Clinical Periodontology*. 2000;27(8):578-589. doi:10.1034/j.1600-051x.2000.027008578.x
12. Bollen CML, Vandekerckhove BNA, Papaioannou W, Van Eldere J, Quirynen M. Full- versus partial-mouth disinfection in the treatment of periodontal infections. *Journal of Clinical Periodontology*. 1996;23(10):960-970. doi:10.1111/j.1600-051x.1996.tb00519.x
13. Yeom HR, Park YJ, Lee SJ, Rhyu IC, Chung CP, Nisengard RJ. Clinical and microbiological effects of minocycline-loaded microcapsules in adult periodontitis. *Journal of Periodontology*. 1997;68(11):1102-1109. doi:10.1902/jop.1997.68.11.1102
14. Quirynen M, Bollen CM, Papaioannou W, Van Eldere J, van Steenberghe D. The influence of titanium abutment surface roughness on plaque accumulation and gingivitis: short-term observations. *The International Journal of Oral & Maxillofacial Implants*. 1996;11(2):169-178.
15. Acharya S, Goyal A, Utreja AK, Mohanty U. Effect of three different motivational techniques on oral hygiene and gingival health of patients undergoing multibracketed orthodontics. *The Angle Orthodontist*. 2011;81(5):884-888. doi:10.2319/112210-680.1
16. Gallie A. Home use of interdental cleaning devices and toothbrushing and their role in disease prevention. *Evidence-Based Dentistry*. 2019;20(4):103-104. doi:10.1038/s41432-019-0069-7
17. Goyal CR, Lyle DM, Qaqish JG, Schuller R. The addition of a water flosser to power tooth brushing: effect on bleeding, gingivitis, and plaque. *The Journal of Clinical Dentistry*. 2012;23(2):57-63.
18. Tawakoli PN, Sauer B, Becker K, Buchalla W, Attin T. Interproximal biofilm removal by intervallic use of a sonic toothbrush compared to an oral irrigation system. *BMC Oral Health*. 2015;15(1). doi:10.1186/s12903-015-0079-6
19. Eakle WS, Ford C, Boyd RL. Depth of penetration in periodontal pockets with oral irrigation. *Journal of Clinical Periodontology*. 1986;13(1):39-44. doi:10.1111/j.1600-051x.1986.tb01412.x
20. Cutler CW, Stanford TW, Abraham C, Cederberg RA, Boardman TJ, Ross C. Clinical benefits of oral irrigation for periodontitis are related to reduction of pro-inflammatory cytokine levels and plaque. *Journal of Clinical Periodontology*. 2000;27(2):134-143. doi:10.1034/j.1600-051x.2000.027002134.x
21. Costa FO, Costa AA, Cota LOM. The use of interdental brushes or oral irrigators as adjuvants to conventional oral hygiene associated with recurrence of periodontitis in periodontal maintenance therapy: A 6-year prospective study. *Journal of Periodontology*. 2019;91(1):26-36. doi:10.1002/jper.18-0637
22. Quirynen M, Teughels W, van Steenberghe D. Impact of antiseptics on one-stage, full-mouth disinfection. *Journal of Clinical Periodontology*. 2006;33(1):49-52. doi:10.1111/j.1600-051x.2005.00868.x

European Journal of Musculoskeletal Diseases
ISSN 2038-4106/2021

Comparative Study

ROLE OF HYALURONIC ACID IN MESENCHYMAL STEM CELL DIFFERENTIATION: A CELLULAR INVESTIGATION ON INFLAMMATION BIOLOGICAL NETWORK

M. Martinelli[1] and A. Pellati[2]

[1]Department of Experimental, Diagnostic and Specialty Medicine, University of Bologna, Italy
[2]Department of Translational Medicine, University of Ferrara, Ferrara, Italy

Correspondence to:
Marcella Martinelli, PhD
Department of Experimental, Diagnostic and Specialty Medicine,
University of Bologna, Bologna, Italy
e-mail: marcella.martinelli@unibo.it

ABSTRACT

Hyaluronic acid (HA) is the major structural component of the extracellular matrix, involved in signaling pathways, inflammation, wound repair, and morphogenesis.

HA is considered an important biomaterial for tissue engineering, drug delivery systems and various medical and pharmaceutical applications based on its characteristics, such as its good biocompatibility, biodegradability, and viscoelastic properties. The physiological properties of HA largely depend on its molecular weight and ability to interact with specific cell receptors.

In this study, we evaluated the correlation between the molecular weight and physiological function of HA by measuring the expression of some inflammatory mediators, such as cytokines, chemokines, and interleukins in mesenchymal stem cells.

Gene expression of genes belonging to the "Inflammatory Cytokines and Receptors" pathway was measured by Real-Time PCR after 24h of treatment with high, medium, and low molecular weight HA solution.

The results confirm the anti-inflammatory activity of high molecular weight HA and the pro-inflammatory and immuno-stimulating activity of medium and low molecular weight HA.

KEYWORDS: *Hyaluronic acid, inflammation, mesenchymal stem cells, real-time PCR*

INTRODUCTION

Hyaluronic acid (HA) is a linear polymer belonging to the family of unbranched polysaccharides called glycosaminoglycans (GAGs), composed of repeated disaccharide units of β-1, 3-N-acetyl-D-glucosamine, and β-1, 4

Received: 12 January 2021
Accepted: 17 August 2021

ISSN: 2038-4106

acid-glucuronic (1). It is a natural extracellular matrix component found in various body fluids, organs, and tissues. It is found at high levels in the umbilical cord, synovial fluid, skin dermis, epidermis, vitreous of the eye, and blood (2). It is synthesized by fibroblasts, keratinocytes, and endothelial cells in the skin region to regulate various biological processes, including signaling, inflammation, wound repair, morphogenesis, and others (3-5).

The molecular size of HA varies from 0.8 kDa to 3000 kDa and is determined by the number of repeated disaccharide units. The biological functions of HA depend on molecular weight. HA with a molecular weight greater than 1000 kDa exerts antiangiogenic, immunosuppressive, and anti-inflammatory effects (6). High molecular weight HA is also highly viscoelastic and viscous and can protect cartilage by acting as a lubricant in the synovial fluid. Conversely, medium and low molecular weight HA possesses pro-inflammatory, pro-angiogenic, and immunostimulating properties (1, 3).

The physiological responses mediated by HA usually correlate with the immune functions that cause inflammation of the tissues and are based on the different molecular sizes related to the different receptors used. Low molecular weight HA binds to toll-like receptor (TLR) 4, an innate bacterial lipopolysaccharide (LPS) receptor, while CD44 glycoprotein is the major high molecular weight HA binding receptor.

HA degradation is mainly mediated by members of a family of enzymes called hyaluronidases (HYAL1 and HYAL2) via the CD44 receptor in macrophages (7, 8). HYAL1 and HYAL2 are the main types of hyaluronidase and are distinguished by their action at the protein level. HYAL2 is responsible for the cleavage of high molecular weight HA, which is mainly bound to the CD44 receptor, where HYAL1 degrades HA in the lysosomes to generate HA oligosaccharides (9).

One of the best-known functions of HA is hydration, thanks to its good ability to trap water (2). Based on its characteristics, such as its good biocompatibility, biodegradability, and viscoelastic properties, HA is considered an important biomaterial for tissue engineering, drug delivery systems, and various medical and pharmaceutical applications (10, 11). HA is also known to reduce the appearance of wrinkles and accelerate wound healing. In addition to these functions, HA-based formulations have shown remarkable efficacy in treating a wide range of inflammatory skin diseases (12-14). In this study, we tested the effects of three different weight hyaluronic acids (high, medium, and low molecular weight) on a population of mesenchymal stem cells isolated from dental pulp.

Mesenchymal stem cells are an excellent model for testing biomaterials' effects or substances' cellular compatibility thanks to their multilineage differentiation potential, high proliferation activity, and self-renewal (15). Moreover, thanks to the ease of availability and isolation, the dental pulp is an excellent source of mesenchymal stem cells (16).

MATERIALS AND METHODS

Dental pulp stem cells isolation

Dental germ pulp was extracted from the third molars of healthy subjects. Pulp was digested for 1 h at 37 °C in a solution containing 3 mg/ml type I collagenase, 4 mg/ml dispase, in 4 ml phosphate-buffered saline (PBS) solution supplemented with 100 U/ml penicillin, 100 µg/ml streptomycin, and 500 µg/ml clarithromycin. The solution was then filtered with 70 µm Falcon strainers (Sigma Aldrich). Filtered cells were cultivated in α-MEM culture medium (Sigma Aldrich) supplemented with 20% FCS, 100 µM 2P-ascorbic acid, 2 mM L-glutamine, 100 U/ml penicillin, 100 µg/ml streptomycin and placed in 25 cm^2 flasks. Flasks were incubated at 37°C, and 5% $CO_{2,}$ and the medium changed twice a week.

Flow cytometric analyses

The purity of dental pulp stem cells (DPSC) cultures was determined by analysis of different antigens after staining with a fluorochrome (FITC- or PE-) conjugated mAbs anti-human CD14-FITC, CD14-PE, CD34-FITC, CD45-FITC, CD90-PE, CD105-PE (Immunotech) and analyzed by FACScan. The nonspecific mouse IgG was used as isotype control (Immunotech). In order to avoid nonspecific fluorescence from dead cells, live cells were gated tightly using forward, and side scatter.

Cell viability test

PrestoBlue™ Reagent Protocol (Invitrogen) was used to evaluate the viability of cells treated with high molecular weight hyaluronic acid (HMW-HA), medium molecular weight hyaluronic acid (MMW-HA), and low molecular weight hyaluronic acid (LMW-HA) solutions at different concentration. A stock solution of 10 g/mL of each molecular weight HA was prepared. Further dilutions were made with the culture medium to the desired concentrations before use.

Serial dilutions of each different molecular weight HA solution (1000 mg/mL, 100 mg/mL, 10 mg/mL, 1 mg/mL) were added (three wells for each concentration). The cell culture medium alone was used as a negative control. Cells were

seeded into 96-well plates at a density of 10^4 cells per well containing 100 µl of cell culture medium. After 24h of incubation, cell viability was measured using PrestoBlue™ reagent protocol. The percentage of viable cells was determined by comparing the average absorbance in drug-treated with average absorbance in control wells exposed to vehicle alone. The results were presented as the mean ± standard deviation of three measures.

Cell treatment

Cells were seeded at a 1.0 x 10^5 cells/ml density into 9 cm^2 (3 ml) wells and subjected to serum starvation for 16 hours at 37°C. After serum starvation, cells were treated with the following solutions: a) 10 mg/mL of HMW-HA; b) 10 mg/mL of MMW-HA; c) 10 mg/mL of LMW-HA. All solutions were obtained in DMEM supplemented with 2% FBS, antibiotics, and amino acids. For each treatment, three biological replicates were performed.

The cells were maintained in a humidified atmosphere of 5% CO_2 at 37°C for 24 hours. Cell medium alone was used as a negative control. After the end of the exposure time, cells were trypsinized and processed for RNA extraction.

RNA isolation, reverse transcription and quantitative real-time RT-PCR

According to the manufacturer's instructions, total RNA was isolated from cell lines using GenElute mammalian total RNA purification miniprep kit (Sigma-Aldrich). Pure RNA was quantified at NanoDrop 2000 spectrophotometer (Thermo Scientific).

Table I. *Selected genes used in Real-Time PCR grouped by functional pathway.*

Phatway	Gene symbol	Gene name
Chemokine	CCL1	C-C motif chemokine ligand 1
	CCL2	C-C motif chemokine ligand 2
	CCL2D	C-C motif chemokine ligand 2 D
	CCL5	C-C motif chemokine ligand 5
	CCL8	C-C motif chemokine ligand 8
	CXCL5	C-X-C motif chemokine ligand 5
	CXCL10	C-X-C motif chemokine ligand 10
Chemokine receptor	CCR1	C-C motif chemokine receptor 1
	CCR2	C-C motif chemokine receptor 2
	CCR5	C-C motif chemokine receptor 5
	CCR6	C-C motif chemokine receptor 6
	CCR10	C-C motif chemokine receptor 10
	CXCR5	C-X-C motif chemokine receptor 5
Interleukin	IL1A	interleukin 1 alpha
	IL1B	interleukin 1 beta
	IL2	interleukin 2
	IL3	interleukin 3
	IL5	interleukin 5
	IL6	interleukin 6
	IL7	interleukin 7
	IL8	interleukin 8
Interleukin receptor	ILR1	interleukin 1 receptor type 1
	IL1RN	interleukin 1 receptor antagonist
	IL6R	interleukin 6 receptor
	IL10RB	interleukin 10 receptor subunit beta
Cytokine	BMP2	bone morphogenetic protein 2
	SPP1	secreted phosphoprotein 1
	TNFSF10	TNF superfamily member 10
	TNFSF11	TNF superfamily member 11
	VEGFA	vascular endothelial growth factor A
Cytokine receptor	TNFRSF	tumor necrosis factor receptor superfamily
Reference gene	RPL13	ribosomal protein L13

cDNA synthesis was performed starting from 500 ng of total RNA, using PrimeScript RT Master Mix (Takara Bio Inc.). The reaction was incubated at 37 °C for 15 min and inactivated by heating at 70 °C for 10 sec. cDNA was amplified by Real-Time Quantitative PCR using the ABI PRISM 7500 (Applied Biosystems).

All PCR reactions were performed in a 20 µl volume. Each reaction contained 10 µL of 2x qPCRBIO SYGreen Mix Lo-ROX (Pcrbiosystems), 400 nM concentration of each primer, and cDNA. Custom primers belonging to the "Inflammatory Cytokines and Receptors" pathway were purchased from Sigma Aldrich. The selected genes grouped by functional pathway are listed in Table I.

All experiments were performed, including non-template controls, to exclude reagent contamination. PCR was performed, including two analytical replicates. The amplification profile was initiated by 10 minutes of incubation at 95°C, followed by two-step amplification of 15 seconds at 95 °C and 60 seconds at 60 °C for 40 cycles. As a final step, a melt curve dissociation analysis was performed.

Statistical analysis

The gene expression levels were normalized to the expression of the reference gene (RPL13) and were expressed as fold changes relative to the expression of the untreated cells. Quantification was done with the delta/delta Ct calculation method (17).

RESULTS

DPSC was treated with three different dilutions of hyaluronic acid stock solutions (high, medium, and low molecular weight) to establish the correct concentration to be used in the treatment of cells cultured *in vitro*. After 24 hours of treatment, cell viability was measured using the PrestoBlue™ assay establishing that the optimal concentration of the treatment that did not significantly affect cell viability was 10 mg/ml for all three types of hyaluronic acid.

Gene expression of genes belonging to the "Inflammatory Cytokines and Receptors" pathway was measured by Real-Time PCR in DPSC treated with high, medium, and low molecular weight hyaluronic acid solution 10 mg/ml for 24 h hours. Table II shows significant gene expression levels after 24 hours of treatment with high molecular weight hyaluronic acid (HMW-HA) compared to untreated cells.

Table II. *Significant gene expression levels after 24h treatment with HMW-HA, as compared with untreated cells.*

Gene	Fold change	SD (+/-)	Gene function
CCL1	3.24	1.19	Chemokine
CCL2	0.41	0.05	Chemokine
CCL2D	0.40	0.08	Chemokine
CCL8	0.14	0.00	Chemokine
CXCL5	0.13	0.04	Chemokine
CXCL10	0.30	0.01	Chemokine
CCR2	0.14	0.00	Chemokine receptor
CCR5	0.17	0.00	Chemokine receptor
CCR6	0.09	0.02	Chemokine receptor
CXCR5	0.23	0.03	Chemokine receptor
IL2	0.15	0.03	Interleukin
IL3	0.24	0.03	Interleukin
IL5	0.04	0.01	Interleukin
TNFRSF	0.22	0.04	Cytokine receptor
TNFSF11	0.26	0.01	Cytokine

All the significantly deregulated genes, except the chemokine CCL1, were down-regulated in treated cells. Genes were "Chemokine" (CCL2, CCL2D, CCL8, CXCL5, CXCL10), "Chemokine receptor" (CCR2, CCR5, CCR6, CXCR5), "Interleukin" (IL2, IL3, IL5), "Cytokine" (TNFSF11) and "Cytokine receptor" (TNFRSF). Fig. 1 represents the gene expression profile of treated stem cells compared with control (untreated cells).

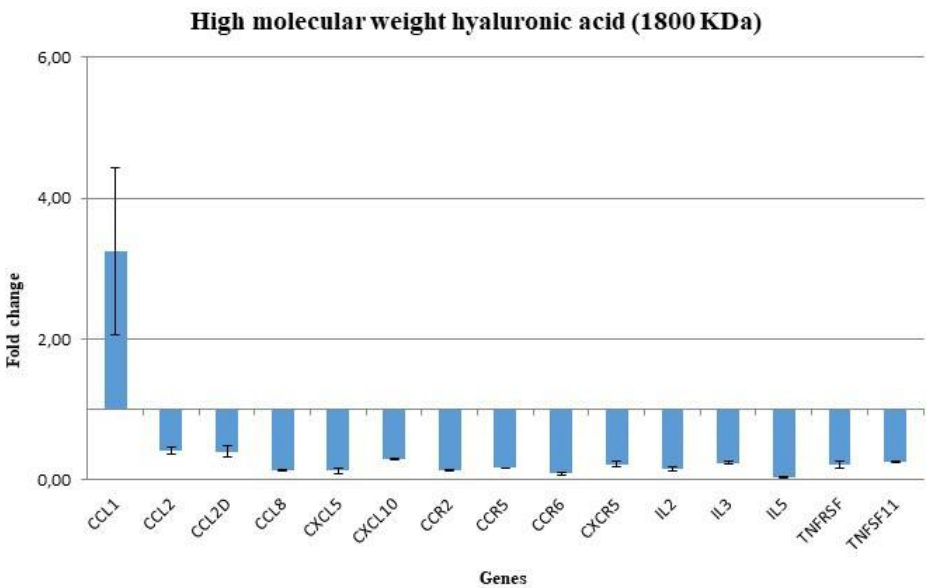

Fig. 1. *Gene expression profile of human DPSC treated with HMW-HA 10 mg/ml.*

Table III reported the significant gene expression levels after 24h treatment with medium molecular weight hyaluronic acid (MMW-HA) compared to untreated cells. The treatment induces the down-regulation of genes belonging to "Chemokine" (CCL1, CCL2, CCL2D, CCL8, CXCL5, CXCL10), "Chemokine receptor" (CCR1, CCR2, CCR4, CCR5, CCR6, CXCR5), "Interleukin" (IL2 and IL5), "Interleukin receptor" (IL1RN), "Cytokine" (SPP1, TNFSF11) and "Cytokine receptor" (TNFRSF). Only three genes, the chemokine CCL5 and the interleukins IL1A and IL6 were significantly up-regulated, as shown in Fig. 2.

Table IV reported the significant gene expression levels after 24h treatment with low molecular weight hyaluronic acid (LMW-HA) compared to untreated cells. Significantly up-regulated genes were chemokine CCL1 and chemokine receptor CCR10, interleukins IL1A, IL5 and interleukin receptor IL6R, cytokines SPP1 and TNFSF11. Conversely, among the down-regulated genes after treatment, there were chemokines CCL2 and CXCL10, chemokine receptors CCR1 and CCR2, and interleukin receptor ILR1. Fig. 3 shows the expression profile of genes up-and down-regulated in stem cells treated with low molecular weight hyaluronic acid.

Table III. *Significant gene expression levels after 24h treatment with MMW-HA, as compared with untreated cells.*

Gene	Fold change	SD (+/-)	Gene function
CCL1	0.09	0.01	Chemokine
CCL2	0.21	0.01	Chemokine
CCL2D	0.49	0.02	Chemokine
CCL5	2.92	0.33	Chemokine
CCL8	0.15	0.01	Chemokine
CXCL5	0.22	0.02	Chemokine
CXCL10	0.10	0.01	Chemokine
CCR1	0.19	0.02	Chemokine receptor
CCR2	0.06	0.00	Chemokine receptor
CCR4	0.10	0.03	Chemokine receptor
CCR5	0.32	0.01	Chemokine receptor
CCR6	0.19	0.02	Chemokine receptor
CXCR5	0.34	0.05	Chemokine receptor
IL1A	2.57	0.01	Interleukin
IL2	0.21	0.06	Interleukin
IL5	0.18	0.01	Interleukin
IL6	3.70	0.14	Interleukin
IL1RN	0.48	0.04	Interleukin receptor
SPP1	0.43	0.01	Cytokine
TNFRSF	0.33	0.01	Cytokine receptor
TNFSF11	0.17	0.17	Cytokine

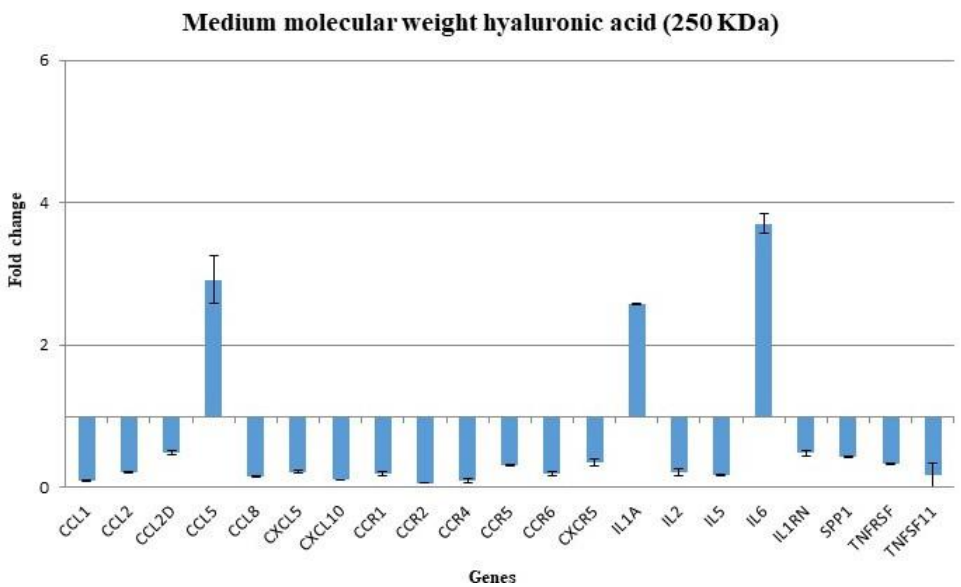

Fig. 2. *Gene expression profile of human DPSC treated with MMW-HA 10 mg/ml.*

DISCUSSION

HA is a linear glycosaminoglycan composed of alternating units of β-1,4-bonded D-glucuronic acid and β-1-3-bonded N-acetyl-D-glucosamine-linked and synthesized by fibroblasts, keratinocytes and endothelial cells (18). It is the major structural component of the extracellular matrix, involved in signaling pathways, inflammation, wound repair, and morphogenesis (3). Numerous studies have highlighted how the physiological properties of hyaluronic acid largely depend on its molecular weight and ability to interact with specific cell receptors (3, 19). High molecular weight hyaluronic acid interacts with the CD44 receptor and has antiangiogenic, immunosuppressive, and anti-inflammatory effects (6). Low molecular weight HA, in contrast, binds to the toll-like rector (TLR) 4, an innate bacterial lipopolysaccharide (LPS) receptor, and possesses pro-inflammatory, pro-angiogenic, and immunostimulating properties (20, 21).

Table IV. *Significant gene expression levels after 24h treatment with LMW-HA, as compared with untreated cells.*

Gene	Fold change	SD (+/-)	Gene function
CCL1	2.35	0.55	Chemokine
CCL2	0.21	0.04	Chemokine
CXCL10	0.17	0.04	Chemokine
CCR1	0.42	0.08	Chemokine receptor
CCR2	0.41	0.04	Chemokine receptor
CCR10	2.29	0.17	Chemokine receptor
IL1A	2.39	0.40	Interleukin
IL5	2.24	0.15	Interleukin
ILR1	0.48	0.13	Interleukin receptor
IL6R	2.03	0.36	Interleukin receptor
SPP1	2.97	0.27	Cytokine
TNFSF11	2.91	0.50	Cytokine

In this study, we evaluated the correlation between HA's molecular weight and physiological function by measuring the expression of some inflammatory mediators, such as cytokines, chemokines, and interleukins, in mesenchymal stem cells extracted from the dental pulp after 24 hours of treatment with HA.

Gene expression levels of genes belonging to the "Inflammatory Cytokines and Receptors" pathway were measured by Real-Time PCR. All the genes (except the cytokine CCL1) expressing pro-inflammatory mediators were significantly down-regulated by treatment of cells with HMW-HA, confirming this polymer's anti-inflammatory and restorative activity at the high molecular weight.

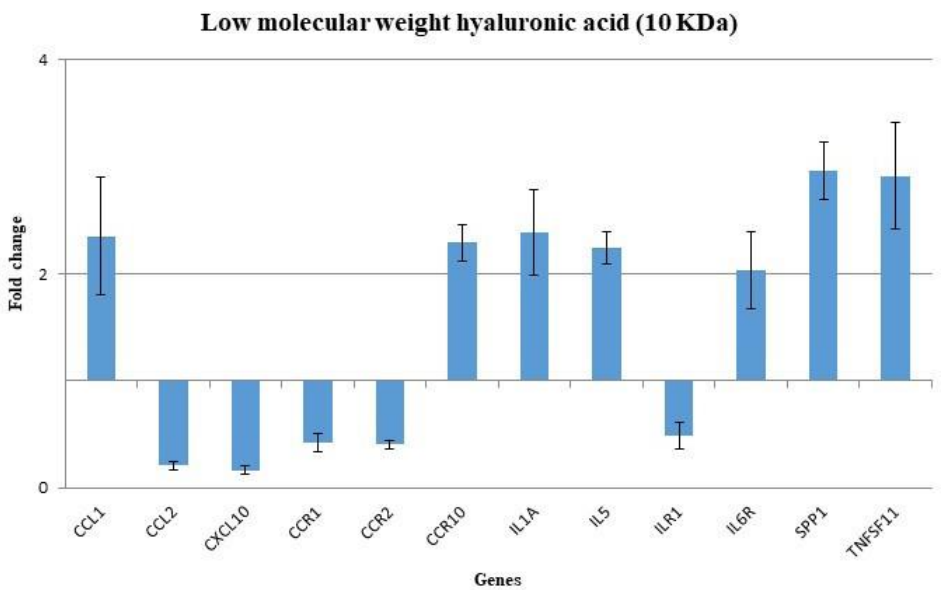

Fig. 3. *Gene expression profile of human DPSC treated with LMW-HA 10 mg/ml.*

Instead, treatment with medium and low molecular weight HA seems to confirm the pro-inflammatory and immunostimulating properties exerted by low and medium molecular weight HA. Stem cells treated with MMW-HA showed significant over-expression of pro-inflammatory interleukins such as IL1A and IL6; this trend becomes more evident in the treatment with LMW-HA, where in addition to the overexpression of interleukins IL1A, IL5 and IL6, up-regulation of cytokines SPP1 and TNSF11, were also observed.

Both medium and low molecular weight HA treatments induce significant over-expression of IL6. LMW-HA binds to toll-like receptor (TLR) 4, activating nuclear factor kappa B (NF-κB) via a myeloid differentiation factor (MyD) 88 dependent pathway leading to nuclear translocation of NF-κB to induce cytokine expression pro-inflammatory, such as interleukin 6 (IL-6) (22). The results confirm the anti-inflammatory activity of high molecular weight HA and the pro-inflammatory and immuno-stimulating activity of medium and low molecular weight HA.

REFERENCES

1. Gall Y. Acide hyaluronique : structure, métabolisme et implication dans la cicatrisation. *Annales de Dermatologie et de Vénéréologie*. 2010;137:S30-S39. doi:10.1016/s0151-9638(10)70007-7
2. Papakonstantinou E, Roth M, Karakiulakis G. Hyaluronic acid: A key molecule in skin aging. *Dermato-Endocrinology*. 2012;4(3):253-258. doi:10.4161/derm.21923
3. Litwiniuk M, Krejner A, Speyrer MS, Gauto AR, Grzela T. Hyaluronic Acid in Inflammation and Tissue Regeneration. *Wounds: A Compendium of Clinical Research and Practice*. 2016;28(3):78-88.
4. Olczyk P, Komosińska-Vassev K, Winsz-Szczotka K, Kuźnik-Trocha K, Olczyk K. [Hyaluronan: structure, metabolism, functions, and role in wound healing]. *Postepy Higieny I Medycyny Doswiadczalnej (Online)*. 2008;62:651-659.
5. Slevin M, Krupinski J, Gaffney J, et al. Hyaluronan-mediated angiogenesis in vascular disease: Uncovering RHAMM and CD44 receptor signaling pathways. *Matrix Biology*. 2007;26(1):58-68. doi:10.1016/j.matbio.2006.08.261
6. Rayahin JE, Buhrman JS, Zhang Y, Koh TJ, Gemeinhart RA. High and low molecular weight hyaluronic acid differentially influence macrophage activation. *ACS biomaterials science & engineering*. 2015;1(7):481. doi:10.1021/acsbiomaterials.5b00181
7. Stern R. Hyaluronan catabolism: a new metabolic pathway. *European Journal of Cell Biology*. 2004;83(7):317-325. doi:10.1078/0171-9335-00392
8. Harada H, Takahashi M. CD44-dependent Intracellular and Extracellular Catabolism of Hyaluronic Acid by Hyaluronidase-1 and -2. *Journal of Biological Chemistry*. 2007;282(8):5597-5607. doi:10.1074/jbc.m608358200
9. Csoka AB, Frost GI, Stern R. The six hyaluronidase-like genes in the human and mouse genomes. *Matrix Biology*. 2001;20(8):499-508. doi:10.1016/s0945-053x(01)00172-x
10. Hong BM, Park SA, Park WH. Effect of photoinitiator on chain degradation of hyaluronic acid. *Biomaterials Research*. 2019;23(1). doi:10.1186/s40824-019-0170-1
11. Lee-Sayer SSM, Dong Y, Arif AA, Olsson M, Brown KL, Johnson P. The Where, When, How, and Why of Hyaluronan Binding by Immune Cells. *Frontiers in Immunology*. 2015;6. doi:10.3389/fimmu.2015.00150
12. Chen LH, Xue JF, Zheng ZY, Shuhaidi M, Thu HE, Hussain Z. Hyaluronic acid, an efficient biomacromolecule for treatment of inflammatory skin and joint diseases: A review of recent developments and critical appraisal of preclinical and clinical investigations. *International Journal of Biological Macromolecules*. 2018;116:572-584. doi:10.1016/j.ijbiomac.2018.05.068
13. Gupta RC, Lall R, Srivastava A, Sinha A. Hyaluronic Acid: Molecular Mechanisms and Therapeutic Trajectory. *Frontiers in Veterinary Science*. 2019;6. doi:10.3389/fvets.2019.00192
14. Salwowska NM, Bebenek KA, Żądło DA, Wcisło-Dziadecka DL. Physiochemical properties and application of hyaluronic acid: a systematic review. *Journal of Cosmetic Dermatology*. 2016;15(4):520-526. doi:10.1111/jocd.12237
15. Lauritano D, Avantaggiato A, Candotto V, et al. Insulin activity on dental pulp stem cell differentiation: an in vitro study. *Journal of Biological Regulators and Homeostatic Agents*. 2015;29(3 Suppl 1):48-53.
16. Mastrolia I, Foppiani EM, Murgia A, et al. Concise Review: Challenges in Clinical Development of Mesenchymal Stromal/Stem Cells. *Stem Cells Translational Medicine*. 2019;8(11). doi:10.1002/sctm.19-0044

17. Livak KJ, Schmittgen TD. Analysis of Relative Gene Expression Data Using Real-Time Quantitative PCR and the 2−ΔΔCT Method. *Methods*. 2001;25(4):402-408. doi:10.1006/meth.2001.1262
18. Dicker KT, Gurski LA, Pradhan-Bhatt S, Witt RL, Farach-Carson MC, Jia X. Hyaluronan: A simple polysaccharide with diverse biological functions. *Acta Biomaterialia*. 2014;10(4):1558-1570. doi:10.1016/j.actbio.2013.12.019
19. Tavianatou AG, Caon I, Franchi M, Piperigkou Z, Galesso D, Karamanos NK. Hyaluronan: molecular size-dependent signaling and biological functions in inflammation and cancer. *The FEBS Journal*. 2019;286(15):2883-2908. doi:10.1111/febs.14777
20. Campo GM, Avenoso A, Campo S, D'Ascola A, Nastasi G, Calatroni A. Molecular size hyaluronan differently modulates toll-like receptor-4 in LPS-induced inflammation in mouse chondrocytes. *Biochimie*. 2010;92(2):204-215. doi:10.1016/j.biochi.2009.10.006
21. Gao Y, Sun Y, Yang H, et al. A Low Molecular Weight Hyaluronic Acid Derivative Accelerates Excisional Wound Healing by Modulating Pro-Inflammation, Promoting Epithelialization and Neovascularization, and Remodeling Collagen. *International Journal of Molecular Sciences*. 2019;20(15):3722. doi:10.3390/ijms20153722
22. Lu YC, Yeh WC, Ohashi PS. LPS/TLR4 signal transduction pathway. *Cytokine*. 2008;42(2):145-151. doi:10.1016/j.cyto.2008.01.006

European Journal of Musculoskeletal Diseases
ISSN 2038-4106/2021

Observational Study

HISTOMORPHOMETRIC ANALYSIS ON SOCKET PRESERVATION IN THE UPPER JAW USING A NEW XENOGRAFT MATERIAL

W. Stablum[1], A. Pellati[2], M. Martinelli[3], F. Lodi[2] and D. Lauritano[2]

[1]Private Practice, Borgo Valsugana (TN), Italy;
[2]Department of Translational Medicine, University of Ferrara, Ferrara, Italy;
[3]Department of Experimental, Diagnostic and Specialty Medicine, University of Bologna, Bologna, Italy

Correspondence to:
Dorina Lauritano, DDS
Department of Translational Medicine, University of Ferrara, 44121 Ferrara, Italy.
e-mail: dorina.lauritano@unife.it

ABSTRACT

After a dental extraction, a variable amount of bone resorption of the residual ridge is observed quantitatively and qualitatively. Alveolar Socket Preservation is a surgical technique that fills alveolar space with biomaterial to maintain alveolar ridge volume for subsequent implant insertion. The purpose of this study is to histologically analyze the healing process of the post-extraction alveoli in the upper jaws grafted with a new biomaterial. Five patients were enrolled in the study, all female, non-smokers, with no periodontal disease or diabetes, and not on any medication. The five treated sites were from three females mean age of 49 years. The two control sites were from two females mean age of 71 years. Test alveoli were packed with decellularized, and antigen-free bovine bone processed at low temperature (RE-BONE®; Ubgen, Padua, Italy) and then covered with a bovine-derived pericardium membrane (SHELTER® FAST; Ubgen, Padua, Italy). At 4 months, surgery for implant insertion was scheduled, and sampling was carried out to obtain bone to be histologically analyzed. The histomorphometric analysis showed an average increase of 6.3% of bone tissue in treated samples compared to controls, but no statistically significant differences were obtained due to the high standard deviation values. In our case series, the new biomaterial shows a good trend as regards the alveolar healing process. However, no conclusion can be drowned due to the limited sample. Therefore, additional studies with greater sample sizes are needed to obtain conclusive results.

KEYWORDS: *bone, graft, alveolus, maxilla, upper jaw*

INTRODUCTION

Alveolar bone is a “tooth-dependent” structure that develops during an eruption, its anatomy (height and thickness) is determined by the formation/presence of the teeth and their axis of eruption.

Received: 28 January 2021
Accepted: 23 March, 2021

ISSN: 2038-4106

Scientific evidence has shown the dynamic change of the tissues after tooth extraction (1, 2). In the first phase after tooth extraction, there is remodelling and resorption of the lingual and buccal walls due to the periodontal ligament's lack of nutritional support. Alveolar bone decreases by about 15% 6 months after extraction (3). Consequently, the size of the socket is reduced both vertically and horizontally. This dimensional change can lead to aesthetic and functional disadvantages, which reflect in a proper subsequent implant insertion. An adequate residual ridge width is one of the main prerogatives for success in long-term implant therapy. In addition, adequate bone volume is required for good soft tissue support (4).

The percentage of alveolar resorption after a tooth extraction is more influenced by bone thicknesses that are greater on the buccal side than on the lingual wall, and consequently, the greatest resorption is found vestibularly. This remodelling occurs in both the lower and upper arches. The most significant contraction occurs during the first month and stabilizes in six months (5).

Schropp et al. (6) studied cases and estimated a loss of ridge width of about 50% over a year. This study highlights the importance of maintaining bone volumes after tooth extraction, especially when dealing with aesthetic areas.

Among the different approaches proposed in the literature to preserve the edentulous ridge, animal-derived biomaterials associated with using barrier membranes were undoubtedly the most analyzed (7). The Alveolar Socket Preservation Technique (ASPT) is a regenerative technique used to minimize the dimensional changes of hard and soft tissues after a dental extraction (8).

ASPT inserts biomaterials in post-extractive alveolus in order to maintain the crest volume. In ASPT, the healing process is similar to that of untreated alveoli (9, 10). The use of membranes to cover the grafted alveolus aim to maintain the biomaterial in situ, or in an ungrafted site, to initially preserve the blood clot, thus excluding its colonization by epithelial cells. Recently a new xenograft has been introduced in the market. The previous report showed that it positively affects alveolus volume maintenance (11, 12).

Here a series of patients were enrolled to be treated with this new biomaterial to maintain crest volume. After 4 months, sapling was performed, and specimens were histologically analyzed to get more information as regards the healing process.

MATERIALS AND METHODS

Five patients who underwent tooth extraction on the upper jaw were enrolled on the study. The reasons for the dental extraction were vertical root fractures, destructive caries, and endodontically non-retractable teeth. All patients were women without periodontal disease or diabetes, non-smokers, and not taking medications such as bisphosphonates or immunosuppressants. The five sites treated with the ASPT were from three patients with a mean age of 49. The two control sites were from two subjects with a mean age of 71.

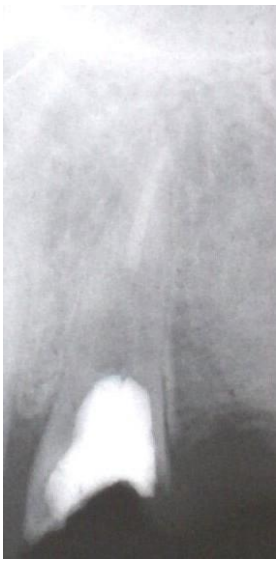

Fig. 1. *Pre-surgical radiograph*

Surgical procedure

During extraction, an attempt was made to lift the flaps in the least invasive way possible to preserve the alveolus bone from further resorption due to surgical exposure. The alveolus was packed with decellularized and antigen-free bovine bone processed at low temperature (RE-BONE®; Ubgen, Padua, Italy) and then covered with a bovine-derived pericardium membrane (SHELTER® FAST; Ubgen, Padua, Italy). The two control sites were treated with the same surgical procedure but without using biomaterials, and the alveoli were left to heal spontaneously (Fig. 1-4).

Compression sutures were performed in monofilament in e-PTFE (Gore-Tex®) and removed after 10 days. An ice pack was maintained for a few hours. Anti-inflammatory therapy with Nimesulide was prescribed as well as soft and cold diet for at least 2/3 days and rinses with Chlorhexidine 2/3 times a day for 15/20 days.

After fourth months, patients were scheduled for implant insertion. Before fixture insertion, sampling was performed using a core drill with a diameter of 2 mm for a depth of 2 mm. The bone samples were placed in sterile and

labelled blisters, immersed in formalin and subsequently sent to the laboratory for histological examination.

Histological analysis

Specimens were treated with Osteosoft® to decalcify the bone samples fixed in formalin. Samples were then embedded in paraffin. A microtome (RM2025 Leica Instruments, Nussloch, Germany) was used to obtain a 5 µm thick section. These paraffin sections, collected on a microscope slide, were deparaffinated, rehydrated, and stained with Haematoxylin and Eosin.

After staining, the sections were dehydrated in alcohol, cleared in xylene, and then preserved using a suitable mounting medium for morphological observations. All reagents were obtained from Sigma-Aldrich.

Histological slides were scanned using an APERIO ScanScope slide scanner (Leica Biosystems, Buccinasco-Milano, Italy), obtaining an image file with .svs (ScanScope Virtual Slide) format for every sample. The .svs files were analyzed using a free software program called ImageScope. The total area of the histological section was measured, as well as the areas occupied by bone and connective tissues.

Fig. 2. *Socket preservation surgery*

RESULTS

Fig. 5 shows histological pictures of test and control specimens. On the left are the areas limited by red and green lines, which correspond to the total sample area and connective tissue area. The bone area is derived from the difference between total and connective tissue areas. The length of the sample, the total area, and the percentage of bone and connective tissues in the scanned histology slides were quantified by ImageScope software.

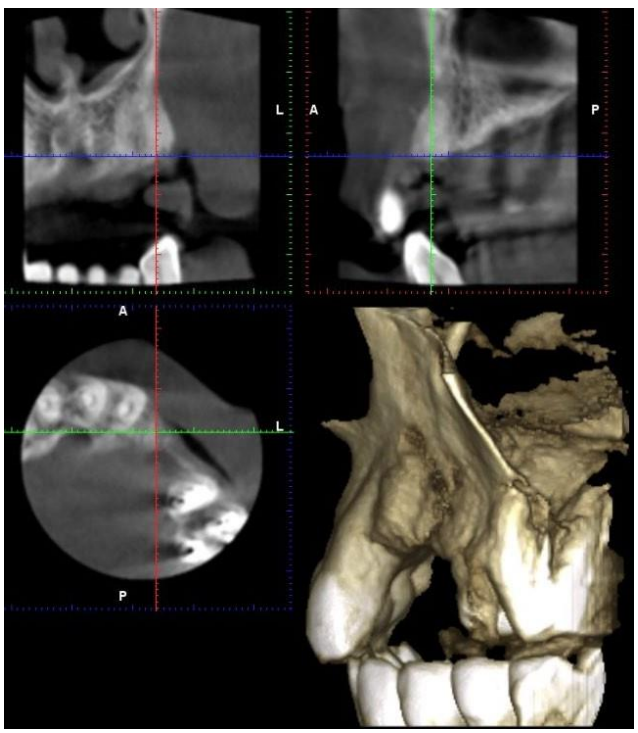

Fig. 3. *Cone beam performed after 4 months of socket preservation*

Fig. 4. *Surgical field just before implant insertion showing the healed alveolus*

Table I reports the average values obtained by all specimens. In treated alveoli, there is an average increase of 6.3% in bone area. Since the standard deviation is similar to the bone gain in the test sample, no statistically significant difference was obtained.

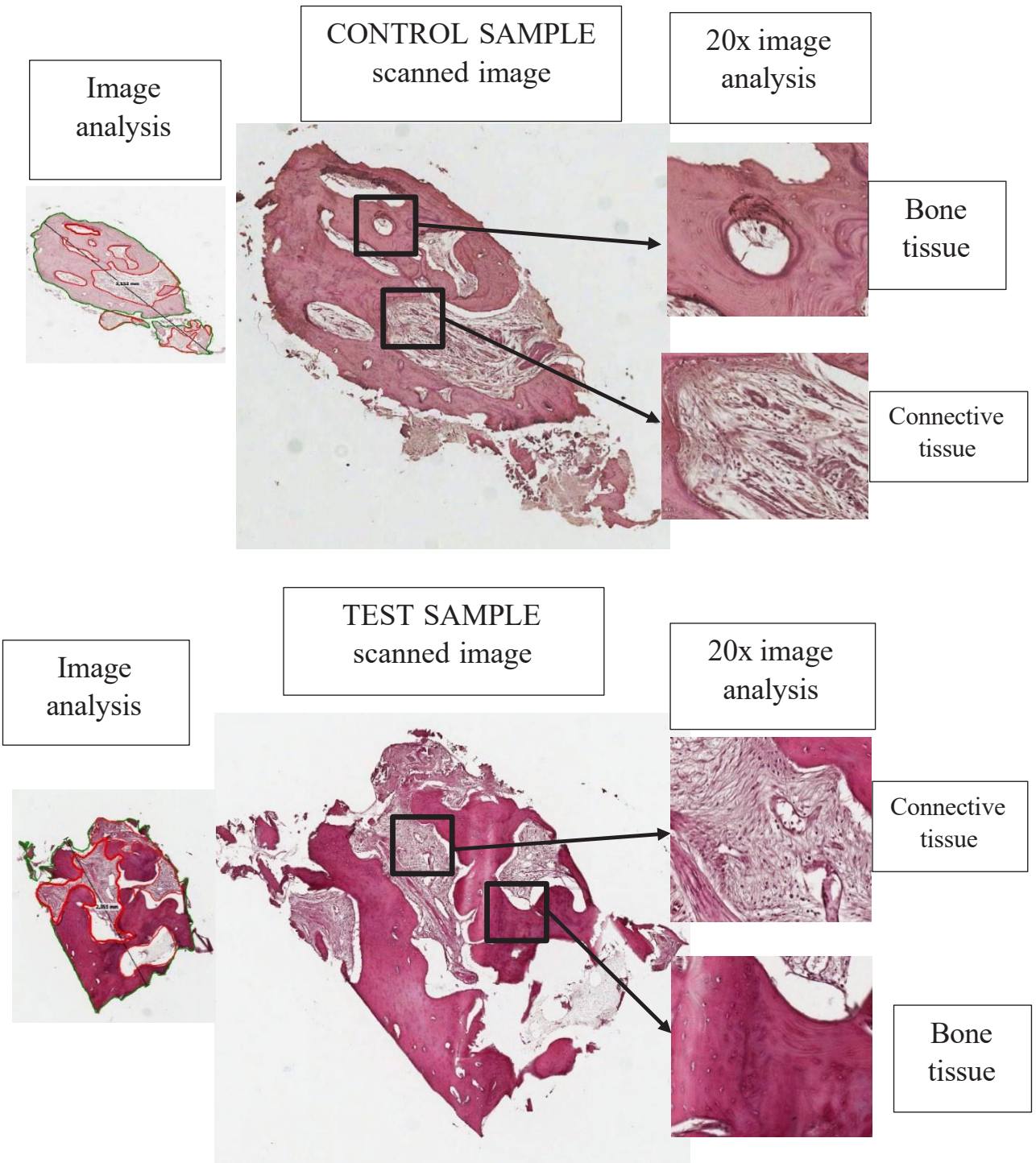

Fig. 5. *Histological and histomorphometric image of a control sample and a test sample.*

Table I. *Average values obtained in bone histomorphometry.*

	Average values				
	Age	Length of samples	Analyzed area	% bone	% connective
Control samples	71.0	3.4 (±0.4)	4.2 (± 2.3)	59.9 (± 5)	40.1 (± 5)
Test samples	49.0	3.8 (±1.94)	5.2 (± 0.8)	66.2 (± 4.96)	33.8 (± 4.96)

DISCUSSION

ASPT is any procedure that takes place immediately after dental extraction to preserve the volume of the alveoli (13). One of the major problems after the extraction of multi-rooted elements in the upper molar area is the loss and/or fracture of the buccal cortex, which makes subsequent management of the implant/prosthetic case much more difficult (14).

Sisti et al. (15) reported that ASPT minimized resorption of the alveolar ridge and provided better regeneration results in sites with buccal bone defects greater than 5 mm compared to the traditional regeneration procedure performed after healing of the socket.

The detachment and careful removal of the granular tissue, combined with a minimally invasive extraction to reduce trauma to the alveolar bone, is of paramount importance to obtain good results with ASPT (16).

The problem of the loss of the vestibular cortex can be attributed to various factors such as trauma, alveolar dehiscence, fracture during avulsion manoeuvres and endodontic infections; to minimize the number of variables, patients without periodontal disease were enrolled in the present study.

Until now, most human studies on ASPT focus on molars extracted for severe periodontitis (17, 18). For example, a study by Rasperini et al. (19), conducted in the posterior area, reported only data for preserved alveoli with four intact walls, while Zhao et al. (20) evaluated only sites in anterior areas.

Carmagnola and coll. (21) performed a study using Bio-Gide® and Bio-Oss® (Geistlich Pharma AG, Switzerland). They divided patients into 3 groups and did histological examinations at 4-7-12 months. At 4 months, connective tissue was present in the membrane graft group, and 40% of the newly formed bone was around the biomaterial.

Cardaropoli et al. (22), in a randomized study, showed that the ASPT group has a significant minor reduction in width and height of the buccal bone crest with respect to the control group with the following values: 1.04 ± 1.08 mm vs 4.48 ± 0.65 mm in with, and 0.46 ± 0.46 mm vs 1.54 ± 0.33 mm in height.

Lee et al. (23) confirmed the potential of ASPT in areas where the vestibular cortex had been compromised. Tomasi et al. (24) stated that if the buccal cortex maintained a thickness greater than 1 mm after extraction, ASPT is unnecessary, while it is indispensable when the thickness of bone is lower.

Since a new biomaterial has been recently introduced in the marker and partially investigated (11, 12), we decided to perform a study to evaluate histological healing of post-extractive sites in the upper molar region. Our results show that in treated alveoli, there is an average increase of 6.3% in bone tissue. However, no statistically significant difference is obtained since the standard deviation is as great as to the bone gain in the test sample.

CONCLUSIONS

Alveolar volume preservation is of paramount importance to have a subsequent proper implant rehabilitation. ASPT is a well-known technique. In addition, various biomaterials are available on the market. Here we investigated a new xenograft inserted in the upper molar area.

From a histological point of view, the healing process has a favourable course with slight increases in bone deposition compared to untreated sites. However, no statistically significant difference was obtained due to the great standard deviation. Furthermore, it is due to the small sample size. Therefore, we believe that additional studies with greater sample sizes are needed to obtain definitive results.

Acknowledgement

Thanks to Maura Boggian for scientific support.

REFERENCES

1. Pietrokovski J, Massler M. Alveolar ridge resorption following tooth extraction. *The Journal of Prosthetic Dentistry*. 1967;17(1):21-27. doi:10.1016/0022-3913(67)90046-7
2. Trombelli L, Farina R, Marzola A, Bozzi L, Liljenberg B, Lindhe J. Modeling and remodeling of human extraction sockets. *Journal of Clinical Periodontology*. 2008;35(7):630-639. doi:10.1111/j.1600-051x.2008.01246.x
3. Cardaropoli G, Araujo M, Lindhe J. Dynamics of bone tissue formation in tooth extraction sites. An experimental study in dogs. *Journal of Clinical Periodontology*. 2003;30(9):809-818. doi:10.1034/j.1600-051x.2003.00366.x
4. Araújo MG, Lindhe J. Dimensional ridge alterations following tooth extraction. An experimental study in the dog. *Journal of Clinical Periodontology*. 2005;32(2):212-218. doi:10.1111/j.1600-051X.2005.00642.x
5. Lekovic V, Kenney EB, Weinlaender M, et al. A bone regenerative approach to alveolar ridge maintenance following tooth extraction. Report of 10 cases. *Journal of Periodontology*. 1997;68(6):563-570. doi:10.1902/jop.1997.68.6.563
6. Schropp L, Wenzel A, Kostopoulos L, Karring T. Bone healing and soft tissue contour changes following single-tooth extraction: a clinical and radiographic 12-month prospective study. *The International Journal of Periodontics & Restorative Dentistry*. 2003;23(4):313-323.
7. Engler-Hamm D, Cheung WS, Yen A, Stark PC, Griffin T. Ridge Preservation Using a Composite Bone Graft and a Bioabsorbable Membrane With and Without Primary Wound Closure: A Comparative Clinical Trial. *Journal of Periodontology*. 2011;82(3):377-387. doi:10.1902/jop.2010.090342
8. Dimova C. Socket Preservation Procedure after Tooth Extraction. *Key Engineering Materials*. 2013;587:325-330. doi:10.4028/www.scientific.net/KEM.587.325
9. Cardaropoli D, Cardaropoli G. Preservation of the postextraction alveolar ridge: a clinical and histologic study. *The International Journal of Periodontics & Restorative Dentistry*. 2008;28(5):469-477.
10. Barone A, Aldini NN, Fini M, Giardino R, Calvo Guirado JL, Covani U. Xenograft Versus Extraction Alone for Ridge Preservation After Tooth Removal: A Clinical and Histomorphometric Study. *Journal of Periodontology*. 2008;79(8):1370-1377. doi:10.1902/jop.2008.070628
11. Gardin C, Ricci S, Ferroni L, et al. Decellularization and Delipidation Protocols of Bovine Bone and Pericardium for Bone Grafting and Guided Bone Regeneration Procedures. *PLOS ONE*. 2015;10(7):e0132344. doi:10.1371/journal.pone.0132344
12. Ludovichetti F, Ludovichetti M. Utilizzo di osso bovino decellularizzato e delipidato e di una membrana in pericardio per la rigenerazione di alveoli post-estrattivi e successiva riabilitazione implanto-protesica: risultati clinici e istologici. *Dental Tribune Italy*. Published online April 14, 2020.
13. Tomasi C, Tessarolo F, Caola I, et al. Early healing of peri-implant mucosa in man. *Journal of Clinical Periodontology*. 2016;43(10):816-824. doi:10.1111/jcpe.12591
14. Tan WL, Wong TLT, Wong MCM, Lang NP. A systematic review of post-extractional alveolar hard and soft tissue dimensional changes in humans. *Clinical Oral Implants Research*. 2011;23(Suppl 5):1-21. doi:10.1111/j.1600-0501.2011.02375.x
15. Sisti A, Canullo L, Mottola MP, Covani U, Barone A, Botticelli D. Clinical evaluation of a ridge augmentation procedure for the severely resorbed alveolar socket: multicenter randomized controlled trial, preliminary results. *Clinical Oral Implants Research*. 2011;23(5):526-535. doi:10.1111/j.1600-0501.2011.02386.x
16. Hong B, Bulsara Y, Gorecki P, Dietrich T. Minimally invasive vertical versus conventional tooth extraction. *The Journal of the American Dental Association*. 2018;149(8):688-695. doi:10.1016/j.adaj.2018.03.022
17. Yang J, Lee HM, Vernino A. Ridge preservation of dentition with severe periodontitis. *Compendium of Continuing Education in Dentistry*. 2000;21(7):579-583; quiz 584.
18. Koo T, Song YW, Cha J, Jung U, Kim C, Lee J. Histologic analysis following grafting of damaged extraction sockets using deproteinized bovine or porcine bone mineral: A randomized clinical trial. *Clinical Oral Implants Research*. 2019;31(1):93-102. doi:10.1111/clr.13557
19. Rasperini G, Canullo L, Dellavia C, Pellegrini G, Simion M. Socket grafting in the posterior maxilla reduces the need for sinus augmentation. *The International Journal of Periodontics & Restorative Dentistry*. 2010;30(3):265-273.

20. Zhao L, Xu T, Hu W, Chung KH. Preservation and augmentation of molar extraction sites affected by severe bone defect due to advanced periodontitis: A prospective clinical trial. *Clinical Implant Dentistry and Related Research*. 2018;20(3):333-344. doi:10.1111/cid.12585
21. Carmagnola D, Adriaens P, Berglundh T. Healing of human extraction sockets filled with Bio-OssR. *Clinical Oral Implants Research*. 2003;14(2):137-143. doi:10.1034/j.1600-0501.2003.140201.x
22. Cardaropoli D, Tamagnone L, Roffredo A, Gaveglio L, Cardaropoli G. Socket preservation using bovine bone mineral and collagen membrane: a randomized controlled clinical trial with histologic analysis. *The International Journal of Periodontics & Restorative Dentistry*. 2012;32(4):421-430.
23. Lee JS, Choe SH, Cha JK, Seo GY, Kim CS. Radiographic and histologic observations of sequential healing processes following ridge augmentation after tooth extraction in buccal-bone-deficient extraction sockets in beagle dogs. *Journal of Clinical Periodontology*. 2018;45(11):1388-1397. doi:10.1111/jcpe.13014
24. Tomasi C, Donati M, Cecchinato D, Szathvary I, Corrà E, Lindhe J. Effect of socket grafting with deproteinized bone mineral: An RCT on dimensional alterations after 6 months. *Clinical Oral Implants Research*. 2018;29(5):435-442. doi:10.1111/clr.13141

European Journal of Musculoskeletal Diseases
ISSN 2038-4106/2021

Evaluation Study

NEW TREATMENT OF CHRONIC VERTEBROGENIC LOW BACK PAIN: THE BASIVERTEBRAL NERVE CT-GUIDED RADIOABLATION

A.E. De Vivo[1], G. D'Agostino[2], G. D'Anna[3], H. Al Qatami[4], I. Gil[5], F. Ventura[1], M. Bonetti[6] and L. Manfrè[1]

[1]Minimal Invasive Spine Department, Mediterranean Institute for Oncology, Viagrande, Catania, Italy;
[2]Nuclear Medicine Department, "Gravina" Hospital, Caltagirone, Catania, Italy;
[3]Radiology Unit, Humanitas Mater Domini, Castellanza, Varese, Italy;
[4]Neuroscience Institution, Hamad General Hospital, Doha, Qatar;
[5]Department of Neuroradiology, Centro Hospitalar Lisboa Ocidental, Lisbon, Portugal;
[6]Department of Neuroradiology, Istituto Clinico Città di Brescia, Brescia, Italy

Correspondence to:
Luigi Manfrè, MD
Mediterranean Institute for Oncology, Corso Italia 10, 95129 Catania, Italy
e-mail: lmanfre@me.com

ABSTRACT

Among the causes of chronic low back pain (LBP), vertebrogenic pain is frequently underestimated. A significant source of LBP is vertebral endplate degeneration, characterized by cortical bone damage and subchondral bone inflammatory reaction. The nerve responsible for pain transmission is the basi-vertebral nerve (BVN). Radiofrequency ablation of the BVN (BVA) leads to thermal injury of nerve tissue and interruption of chronic vertebrogenic pain transmission. The aim of this study is to evaluate the effectiveness, in terms of pain and disability reduction, of percutaneous BVA in the treatment of patients affected by vertebrogenic chronic LBP. A second aim is to assess the feasibility and safety of a percutaneous CT- guided technique. We performed percutaneous CT-guided BVN ablation in 56 consecutive patients presenting with vertebrogenic chronic LBP in local anaesthesia using an articulating bipolar radiofrequency electrode. In order to assess the target success of the procedure, a one-month follow-up MRI was performed to evaluate the ablation area. Three months later, a CT study was performed to evaluate bone mineral density to exclude structural bone abnormalities that the treatment might have induced. Pre-and post-procedure pain and disability levels were measured using the visual analogue scale (VAS) and Oswestry disability index (ODI). A 10-point improvement threshold was set as a clinical success for the ODI score, and a 2cm improvement threshold was set as a clinical success for the VAS score. VAS and ODI scores decreased significantly compared to baseline at 3- and 12-month follow-ups. Clinical success was reached in 54/56 patients (96,5%) for pain and 54/56 patients (96,5%) for disability, exceedingly the "minimum clinically important difference". CT-assisted targeting of the ablation zone was determined successfully in all patients. The mean operative time was 32 minutes. No immediate or delayed complications were detected. Percutaneous CT-guided intra-osseous

Received: 23 January 2021
Accepted: 19 March, 2021

ISSN: 2038-4106

BVA seems to be a safe, fast and powerful technique for pain relief in patients with vertebrogenic chronic LBP when the selection of patients is based on a multidisciplinary approach including both conventional nuclear medicine imaging and diagnostic radiology.

KEYWORDS: *pain, spine, disc, ablation, nerve*

INTRODUCTION

Vertebral endplates are a significant source of lower back pain (LBP): the correlation between vertebral endplate damage with a subchondral bone inflammatory reaction, generally identified as "Modic changes", and LBP has been extensively investigated, and the pathological basis of vertebrogenic LBP in patients with Modic changes yet established (1–6).

The nociceptive role of the basi-vertebral nerve (BVN) is supported by histologic, anatomic and immune-histochemical evidence in the pathogenesis of LBP in patients with Modic type I change: Fras et al. (7) and Bailey et al. (8) identified in the BVN as the source of the intraosseous nerves. The BVN enters the posterior vertebral body via the basivertebral foramen and arborizes near the centre of the vertebral body, receiving branches innervating all the cancellous bone and the superior and inferior endplates (*caput medusae*). Findings prove that these nerve endings proliferate in damaged and degenerated endplates and are more numerous than in normal intervertebral space and disc (9). Fras et al. also reported on the presence of Substance-P within the BVN, concluding that these nerves can potentially transmit pain signals from the vertebral endplates (7).

Radiofrequency (RF) ablation of the BVN is a potential technique for treating vertebrogenic LBP, for it interrupts pain transmission from vertebral endplates. This treatment generates definitive thermal damage of tissue proteins within the coagulation zone adjacent to the conducting region of the RF probe. Histologically this area is characterized by the embolization of blood vessels, the disintegration of neural tissues and the Wallerian degeneration of nerves (10). Coagulation is surrounded by a secondary zone of hyperemia, where there is a local release of inflammatory factors, oedema, and changes in blood flow (11). In the post-op MRI scan, the lesion presents the so-called "bull eye appearance" with two concentric zones on T2-weighted images: a central hyper-intensity area surrounded by a hypo-intense rim. After 12 months of ablation, histological studies from animal model demonstrated: hematopoietic marrow in the zone of coagulation replaced by viable fat; new bone growing on preexisting trabeculae, without evidence of avascular necrosis; rudimentary blood vessels and nerves development at the coagulation zone periphery (12).

Regarding the duration of BVN radiofrequency, its outcome is expected to be long-lasting since the BVN does not appear to regenerate spontaneously: the extent of the thermal injury, combined with the intrinsic anatomical characteristics of the BVN, which is non-myelinated, could explain permanent nerve destruction (13, 14).

The present study aims to evaluate the effectiveness, in terms of pain and disability reduction, of radiofrequency ablation of the BVN (BVA) in the treatment of patients suffering from chronic vertebrogenic LBP. In addition, as a secondary endpoint, the purpose was to assess the feasibility and safety of a percutaneous CT- guided technique.

MATERIALS AND METHOD

Patients with chronic LBP were enrolled; all presented failure of at least 6 weeks of conventional conservative therapies. Exclusion criteria were radicular pain, symptomatic spinal canal stenosis, hemorrhagic diathesis, local or systemic infection and poor compliance. Patients signed informed consent as regards diagnosis, treatment, and scientific purposes.

Based on clinical examination, patients with suspected vertebrogenic LBP underwent conventional lumbar MRI study, including axial and sagittal T1-SE, T2-FSE and T2-STIR weighted images. Patients with MRI signs of subchondral bone inflammatory reaction Modic type I or mixed Modic type I and II underwent lumbar bone SPECT/CT. Patient with evidence of focal vertebral body uptake on SPECT/CT imaging underwent CT-guided medial branch block (MBB) to exclude chronic Facet Joint Syndrome (FJS) with an injection of 1 cc of lidocaine in the area of the zygapophyseal nerve at the presumed level, bilaterally. Patients who did not perceive pain relief after lidocaine MBB were finally considered eligible for percutaneous CT-guided BVA for a total of 56 patients (22 males and 34 females; median age 43 years old,

age range 38-52 years): 18/56 patients had 1 segment affected (6 patients L4; 9 patients L5; 3 patients S1), 38/56 patients had 2 segments affected (13 patients L3-L4; 14 patients L4-L5; 11 patients L5-S1).

All the patients presented disc degeneration classified according to Pfirrmann's grading of lumbar disc degeneration (15); 23/56 with Grade IV; 33/56 with Grade V.

Pre-operative pain intensity was rated by the Visual Analogue Scale (VAS) scale, consisting of a 10cm straight line with defined endpoints ("no pain" and "worst pain imaginable") on which the patients were asked to mark their experienced pain at the actual time ("VAS now"). The VAS is a validated clinical instrument with a high degree of reliability. The Oswestry Disability Index (ODI) score was used to rate the pre-operative back-related disability. ODI is a validated scale of ten questions designed to assess pain intensity and activities of daily living. A 10-point improvement threshold was set as a clinical success for the ODI score, and a 2cm improvement threshold was set as a clinical success for the VAS score. These values correspond to the commonly accepted "minimum clinically important difference" in treating chronic LBP (16, 17). Repeat VAS and ODI measurements were performed at the 3- and 12-month follow-ups.

We performed BVA in 56 consecutive patients by a fully percutaneous procedure using a unique bipolar radiofrequency system with an articulating electrode (STAR®, Merit) which contains two thermocouples embedded along the length of the probe for real-time assessment of the ablation zone size. The proximal thermocouple represents the temperature at the outer margin of the ablation zone. The articulating electrode permits transpedicular access and navigation to the desired location within the vertebral body once beyond the pedicle body junction. With the patients in a prone position on the CT table, 5.0 cc of lidocaine was injected using a 20G spinal needle to obtain local anaesthesia into deep muscle tissue and the periarticular area; using a 10G coaxial needle, a unilateral transpedicular approach was employed to access the vertebral body. In order to prevent thermal injuries to the spinal cord and nerve roots, the distal tip of the access needle was deployed 1cm anterior to the posterior wall of the vertebral body. This location corresponds to the outer margin of the ablation area. The coaxial bone biopsy needle is then introduced, obtaining a bone specimen. An articulating osteotome was then inserted to create a preferential path for optimal positioning of the articulating ablation electrode. The centre of the ablation zone, the radiolucent region of the electrode, was then positioned in the centre of the vertebral body, where most vertebral body nerves cluster. After placing the electrode at the targeted location, thermal ablation was performed

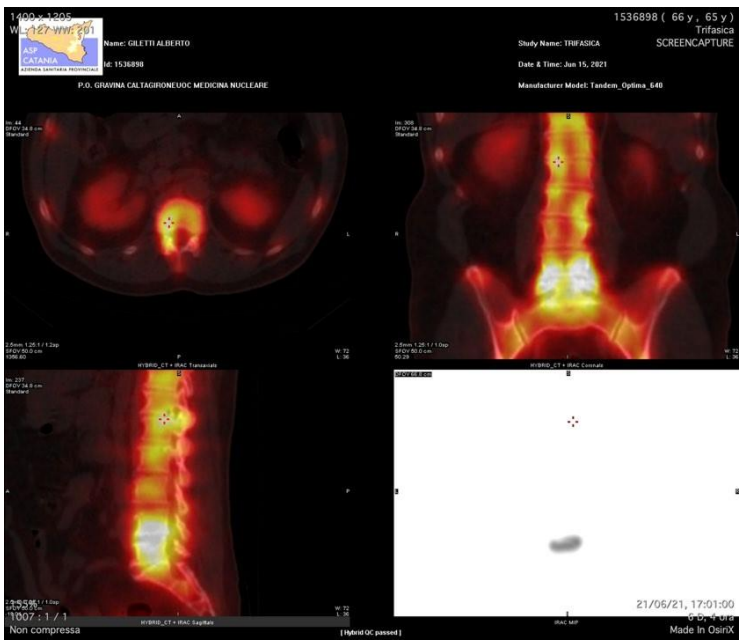

Fig. 1. *66 years male with chronic LBP for 3 years. SPECT-CT on axial, sagittal and coronal recons. Bone scanning clearly depicts severe Tc99 uptake at the L4 and L5 vertebral bodies, confirming the presence of aseptic spondylodiscitis related to chronic mechanical trauma, presumably secondary to disc degeneration.*

using the RF generator until the distal thermocouple reached 55ºC-70ºC, generating a 15 to 20 mm large ablation zone with a core temperature of approximately 77ºC; the RF delivery automatically stopped when the proximal thermocouple reaches 50º C (Fig. 1). The electrode and coaxial needle were then removed, and a post-operative CT performed.
Conventional non-enhanced MRI follow-up studies were performed one month after the procedure, checking for signal abnormality at the level of the endplates and the adjacent intervertebral discs. At the 3-month CT follow-up study, a 0.5 cm^2 "region of interest" (ROI) analysis of the cancellous bone before and after RF ablation was also performed, as well as a comparison between ROI values of the ablated area and the normal non-ablated area in the same vertebral body.

RESULTS

All 56 patients well tolerated the procedure, and no analgo-sedation was necessary. The mean operative time was approximately 32 minutes (range 28-37minutes), with an active ablation time of 5 minutes maximum. No complications occurred at the immediate post-operative CT control scan and the one-month MRI and three-month CT follow-up. Targeting the ablative area was successful in 100% of patients, which consistently included the central portion of the vertebral body along the midline to ensure the BVN ablation. Twelve-month VAS and ODI scores decreased significantly compared to baseline. VAS mean change was -4.3cm (range was -7.5 to -1cm). Clinical success (defined as at least -2.0cm) was achieved in 54/56 patients, in which VAS decreased more than 3.0cm. ODI score meant a change was -32.4 points (range was -6 to -42). Therefore, we decided to evaluate as "clinical success" at least -10 points. This result was achieved in 54/56 patients (96,5%), whose ODI score decreased by more than 20 points. MRI follow-up at 1 month precisely depicts the area of ablation: the centre of the ablated area showed high signal intensity on T2-weighted images, presumably related to a small area of tissue colliquation and necrosis, and a large low signal intensity area, with a concentric reduction in signal intensity, was found both on T1- and T2 weighted scans, related to bone thermal coagulation (Fig. 2). No abnormal signal intensity at the level of adjacent endplates and discs was detected on 1-month MRI follow-up study, excluding presumed vascular damage to the vertebral unit: the endplates remain hypointense on all the sequences, excluding vascular damage or inflammatory-induced reaction at 1 month. No damage was also noted at the level of the disc, both the annulus and the nucleus pulposus.

On the pre-op CT scan, a 0.5cm^2 ROI was placed before treatment on the area to be ablated and the peripheral bone area as an internal control value. This measure was repeated in the same area 3 months after the treatment. Before the treatment, the ROI value of the central core of the vertebral body (the target of the planned RF ablation) was 95.6 Hamsfield Unit (HU – mean value), almost identical to peripheral bone (mean value of 97.3 HU). The 3-month CT

A B

Fig. 2. *66 years male with chronic LBP from 3 years. Sagittal T1SE scan (***A***) and sagittal T2STIR (***B***) images. On MRI a mixed type I and II Modic degeneration can be appreciated at the level of the subcondral somatic bone at L4 and L5, in correspondence to the focal pain referred.*

study demonstrated that the mean bone density value of the ablated area significantly increased to a mean value of 150.9 HU (+57%), while the ROI value of the peripheral cancellous bone area, adjacent to the ablation was not significantly modified (mean value was 96.5HU).

DISCUSSION

The literature shows that Modic changes play an important role in the etiopathogenesis of nonspecific chronic LBP patients (18). Modic type I changes are indicative of oedema and inflammation, the pain being generated by Tumor Necrosis Factors (TNF) release and Protein Gene Products (PGP) (19). In contrast, Modic changes type II are related to bone marrow fatty degeneration, and Modic type III represents sclerosis only as the final evolution of the chronic inflammatory disease. Modic type I changes have a stronger association with pain than Modic II since pain decreases as Modic type I turns into Modic type II (4). Subchondral signal abnormalities represent a dynamic process. Modic type I often converts to Modic type II, but in some cases, lesions can become more extensive or remain unchanged (20-23). Modic type II changes seem to be much more stable, even if there is also some evidence that they may be unstable and change back into type 1 lesions (20-23).

Unfortunately, Modic changes are not an independent and reliable predictor of vertebrogenic chronic LBP and, as for several degenerative changes, are frequently demonstrated on MRI scans in asymptomatic individuals. There is no direct correlation between the size of the Modic type I lesion, clinical presentation, and relevance of LBP or whether recent Modic changes are more symptomatic than longer-lasting ones. Any relationship between symptoms and the duration of such subchondral signal changes remains unknown.

In our study, to confirm the source of chronic LBP in patients with suspected vertebrogenic pain, all participants underwent a SPECT/CT examination (Fig. 3). Bone SPECT/CT is an extremely powerful hybrid imaging system, where SPECT data are merged with conventional CT scans acquired in the same camera. Data from the two modalities are complementary and allow precise localization of the anatomical location of abnormal bone inflammation (24). One of the main advantages of bone SPECT/CT remains the extremely high sensitivity with bone abnormalities becoming apparent earlier than with MRI, CT or any other conventional radiological study. Another SPECT-CT advantage is the capability to image the entire body. Despite the high sensitivity, low SPECT-CT specificity is to be identified as the main drawback: the bone uptake of the tracers, which are usually bisphosphonates labelled with technetium 99m, depends on osteoblast activity and the bone remodelling rate. Therefore, binding is not specific to a specific disease. Consequently, a reliable diagnosis is generally the result of a comparative analysis of CT, MRI and bone scanning (25).

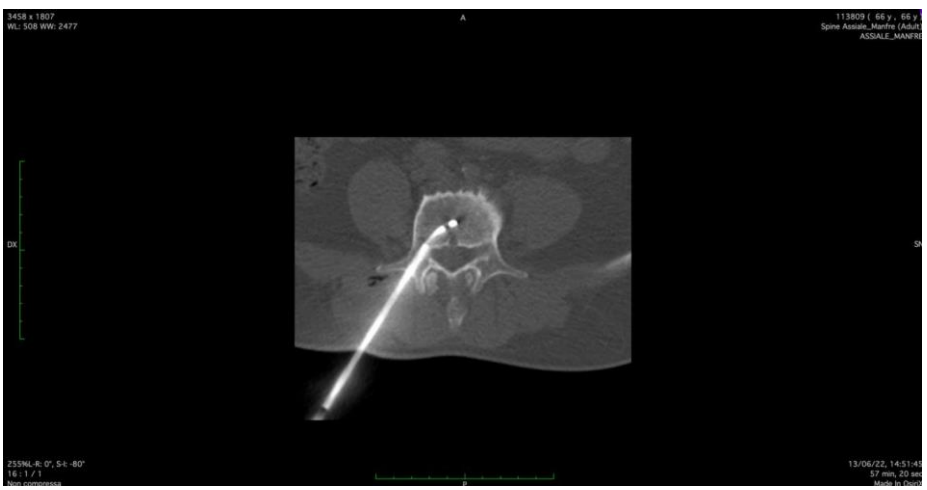

Fig. 3. *66-year-old male with chronic low back pain for 3 years. Basivertebral nerve ablation. CT-guided treatment was performed introducing a steerable radio-probe with a transpeducolar approach inside L4 and L5, reaching the midline at the junction of the anterior 2/3 and posterior 1/3, exactly at the level of the basivertebral nerve rising area.*

In a previous Russo et al. (24) study, the correlation between bone SPECT/CT and Modic changes was investigated. A high positive correlation was found between Modic changes on MRI and increased metabolic activity on bone SPECT/CT imaging. In particular, Modic change type I was the best binary predictor for positivity on bone SPECT/CT. Results showed high metabolic activity in 96.1% of endplates in patients showing Modic type I changes on MRI, 77.8% in cases of Modic type II changes, and only 56% in cases of Modic type III changes. These data suggest that in patients with suspect vertebrogenic pain who might benefit from BVA, the use of bone SPECT/CT compared to conventional MRI for proper selection of patients is a key factor in explaining the high percentage of clinical success obtained.

There are several studies about BVA for the treatment of chronic LBP. However, in all of these studies, the patient selection was made based on MRI imaging only, and results were significantly lower when compared to treatment based on SPECT-CT (24-26).

Moreover, all the BVA treatments in our study were performed using a navigational bipolar RF probe, and CT-guided technique with simultaneous 3D reconstructions obtained intra-operatively so that the best trajectory to the target area in the centre of the vertebra was easily achieved in all cases. Use of a navigational and steerable RF probe permitted safe transpedicular access, trajectory modification once past the pedicle body junction, an action required to reach the target area, and complete ablation of the nerve, reducing the risk of adverse events such as breaching of the pedicle wall and accidental radicular neurovascular thermal injury.

Another issue was the risk of possible damage induced by RF heating transmitted to the peri-ablative area cancellous bone, the endplates and the adjacent disc. For this reason, a 1-month MRI follow-up study and a 3-month CT study were always performed on our population. On the MRI scan, no signal abnormalities were observed at the level of the bone far from the ablated area, the endplates or the adjacent discs, apart from areas through which the probe passed and the target ablation zone. The presumed treatment-related effect on bone integrity was also evaluated by comparing bone mineral density before and 3 months after the procedure: no weakening of the bone was observed. In addition, the results demonstrated sclerosis with an increased bone density of the treated area (+55%) compared to the rest of the vertebral body; this was presumably a result of sclerotic changes induced by the ablation.

All the patients well tolerated conscious sedation using opioids. This technique also reduced any complications related to general anaesthesia.

CONCLUSION

In conclusion, vertebrogenic pain is one of the most frequent and frequently underestimated causes of chronic LBP. The diagnosis cannot rely on CT and/or MRI images alone. Fundamental functional imaging dependent on the metabolic bone activity and SPECT-CT should be considered to increase appropriate patient selection for BVA treatment. Percutaneous CT-guided intra-osseous BVA appears to be a safe, fast and powerful technique for pain relief in patients with vertebrogenic chronic LBP when the selection of patients is based on a multidisciplinary approach, including both conventional diagnostic radiology and bone scanning imaging.

REFERENCES

1. Määttä JH, Wadge S, MacGregor A, Karppinen J, Williams FMK. ISSLS prize winner: Vertebral endplate (modic) change is an independent risk factor for episodes of severe and disabling low back pain. *Spine*. 2015;40(15):1187-1193. doi:10.1097/brs.0000000000000937
2. Luoma K, Vehmas T, Kerttula L, Grönblad M, Rinne E. Chronic low back pain in relation to Modic changes, bony endplate lesions, and disc degeneration in a prospective MRI study. *European Spine Journal*. 2016;25(9):2873-2881. doi:10.1007/s00586-016-4715-x
3. Chung CB, Vande Berg BC, Tavernier T, et al. End plate marrow changes in the asymptomatic lumbosacral spine: frequency, distribution and correlation with age and degenerative changes. *Skeletal Radiology*. 2004;33(7):399-404. doi:10.1007/s00256-004-0780-z

4. Kääpä E, Luoma K, Pitkäniemi J, Kerttula L, Grönblad M. Correlation of Size and Type of Modic Types 1 and 2 Lesions With Clinical Symptoms. *Spine*. 2012;37(2):134-139. doi:10.1097/brs.0b013e3182188a90
5. Albert HB, Manniche C. Modic changes following lumbar disc herniation. *European Spine Journal*. 2007;16(7):977-982. doi:10.1007/s00586-007-0336-8
6. Kjaer P, Korsholm L, Bendix T, Sorensen JS, Leboeuf-Yde C. Modic changes and their associations with clinical findings. *European Spine Journal*. 2006;15(9):1312-1319. doi:10.1007/s00586-006-0185-x
7. Fras C, Kravetz P, Mody DR, Heggeness MH. Substance P-containing nerves within the human vertebral body. an immunohistochemical study of the basivertebral nerve. *The Spine Journal: Official Journal of the North American Spine Society*. 2003;3(1):63-67. doi:10.1016/s1529-9430(02)00455-2
8. Bailey JF, Liebenberg E, Degmetich S, Lotz JC. Innervation patterns of PGP 9.5-positive nerve fibers within the human lumbar vertebra. *Journal of Anatomy*. 2011;218(3):263-270. doi:10.1111/j.1469-7580.2010.01332.x
9. Antonacci MD, Mody DR, Heggeness MH. Innervation of the human vertebral body: a histologic study. *Journal of Spinal Disorders*. 1998;11(6):526-531.
10. Fan KW, Zhu ZX, Den ZY. An experimental model of an electrical injury to the peripheral nerve. *Burns: Journal of the International Society for Burn Injuries*. 2005;31(6):731-736. doi:10.1016/j.burns.2005.02.022
11. Coert JH. Pathophysiology of nerve regeneration and nerve reconstruction in burned patients. *Burns*. 2010;36(5):593-598. doi:10.1016/j.burns.2009.10.007
12. Lotz JC, Fields AJ, Liebenberg EC. The Role of the Vertebral End Plate in Low Back Pain. *Global Spine Journal*. 2013;3(3):153-163. doi:10.1055/s-0033-1347298
13. Sherman M. The Nerves of Bone. *Journal of Bone and Joint Surgery*. 1963;45(3):522-528. doi:10.2106/00004623-196345030-00010
14. Liuzzi FJ, Tedeschi B. Peripheral nerve regeneration. *Neurosurgery Clinics of North America*. 1991;2(1):31-42.
15. Pfirrmann CWA, Metzdorf A, Zanetti M, Hodler J, Boos N. Magnetic Resonance Classification of Lumbar Intervertebral Disc Degeneration. *Spine*. 2001;26(17):1873-1878. doi:10.1097/00007632-200109010-00011
16. Ostelo RWJG, de Vet HCW. Clinically important outcomes in low back pain. *Best Practice & Research Clinical Rheumatology*. 2005;19(4):593-607. doi:10.1016/j.berh.2005.03.003
17. Hägg O, Fritzell P, Nordwall A. The clinical importance of changes in outcome scores after treatment for chronic low back pain. *European Spine Journal*. 2003;12(1):12-20. doi:10.1007/s00586-002-0464-0
18. Carragee EJ, Don AS, Hurwitz EL, Cuellar JM, Carrino J, Herzog R. 2009 ISSLS Prize Winner: Does Discography Cause Accelerated Progression of Degeneration Changes in the Lumbar Disc. *Spine*. 2009;34(21):2338-2345. doi:10.1097/brs.0b013e3181ab5432
19. Rahme R, Moussa R. The Modic Vertebral Endplate and Marrow Changes: Pathologic Significance and Relation to Low Back Pain and Segmental Instability of the Lumbar Spine. *American Journal of Neuroradiology*. 2008;29(5):838-842. doi:10.3174/ajnr.a0925
20. Kuisma M, Karppinen J, Niinimäki J, et al. A Three-Year Follow-up of Lumbar Spine Endplate (Modic) Changes. *Spine*. 2006;31(15):1714-1718. doi:10.1097/01.brs.0000224167.18483.14
21. Mitra D, Cassar-Pullicino VN, Mccall IW. Longitudinal study of vertebral type-1 endplate changes on MR of the lumbar spine. *European Radiology*. 2004;14(9). doi:10.1007/s00330-004-2314-4
22. Luoma K, Vehmas T, Grönblad M, Kerttula L, Kääpä E. Relationship of Modic type 1 change with disc degeneration: a prospective MRI study. *Skeletal Radiology*. 2009;38(3):237-244. doi:10.1007/s00256-008-0611-8
23. Luoma K, Vehmas T, Grönblad M, Kerttula L, Kääpä E. MRI follow-up of subchondral signal abnormalities in a selected group of chronic low back pain patients. *European Spine Journal*. 2008;17(10):1300-1308. doi:10.1007/s00586-008-0716-8
24. Russo VM, Dhawan RT, Dharmarajah N, Baudracco I, Lazzarino AI, Casey AT. Hybrid Bone Single Photon Emission Computed Tomography Imaging in Evaluation of Chronic Low Back Pain: Correlation with Modic Changes and Degenerative Disc Disease. *World Neurosurgery*. 2017;104:816-823. doi:10.1016/j.wneu.2017.03.107

25. Harisankar CNB, Mittal BR, Bhattacharya A, Singh P, Sen R. Utility of single photon emission computed tomography/computed tomography imaging in evaluation of chronic low back pain. *Indian journal of nuclear medicine: IJNM: the official journal of the Society of Nuclear Medicine, India*. 2012;27(3):156-163. doi:10.4103/0972-3919.112720
26. Khalil JG, Smuck M, Koreckij T, et al. A prospective, randomized, multicenter study of intraosseous basivertebral nerve ablation for the treatment of chronic low back pain. *The Spine Journal*. 2019;19(10):1620-1632. doi:10.1016/j.spinee.2019.05.598

European Journal of Musculoskeletal Diseases
ISSN 2038-4106/2021

Letter to the Editor

KOHLER'S BONE DISEASE TYPE 1

V. Sollazzo

Medical Director, Medical Center, Ferrara, Italy

Correspondence to:
Vincenzo Sollazzo, MD
Orthopedic Surgeon, Medical Director, Medical Center, Ferrara, Italy
e-mail: slv@unife.it

ABSTRACT

In 1908, Alban Kohler was the first person to describe the condition now known as Kohler's disease, which is avascular necrosis of the navicular bone in the foot. Kohler's illness is a condition that only affects children and young adults. The navicular bone's pressure before its ossification is assumed to be the root cause of the condition, although its genesis is not completely understood; this results in blood flow irregularities, leading to avascular necrosis. Males between the ages of 4 and 7 are more likely to be affected by Kohler's disease. In most cases, Kohler's disease affects only one side of the body; however, one study indicated that 25% of cases of Kohler's disease affect both sides of the body. Patients will often appear with symptoms including pain on the medial side of the foot, inflammation on the medial foot, and/or a limp. On plain films, the navicular will exhibit typical signs of avascular necrosis, such as sclerosis, disintegration, and flattening of the bone. This condition is caused by the death of blood vessels. The prognosis is very favorable for patients with the self-limiting syndrome known as Kohler's disease. There have been no examples of Kohler's disease that have developed into long-term clinical or radiographic problems recorded.

KEYWORDS: *Kohler's disease; rare bone condition; avascular necrosis*

INTRODUCTION

Kohler's disease is an extremely rare bone condition of the foot that affects children. It is thought that the application of stress-related constriction may cause the condition during a crucial period of the person's development. The limping characteristic of the condition is brought on by swelling and pain in the foot (1). Children between three and seven are most likely to be affected, and boys are five times more likely to be affected than girls. Because the condition only affects one foot at a time, children who have it often walk on the side of their affected foot. The condition seems to go away on its own as children mature, and the bones that are afflicted typically regain their size, strength, and form within three months. Sometimes, patients report symptoms that continue for as long as two years (2).

In 1908, Alban Kohler's was the first person to describe the condition now known as Kohler's disease, which is avascular necrosis (AVN) of the navicular bone in the foot. The Kohler's illness is a condition that only affects children

Received: 19 January 2021
Accepted: 16 aprile 2021

ISSN: 2038-4106

and young adults. The soreness runs particularly down the length of the foot's arch (3). There is a possibility that the affected region will become red. It is difficult to put weight on foot or walk, which causes more agony and a limp. As a result of an interruption in blood flow, the navicular bone gradually deteriorates. However, in a relatively brief period, the bone will heal independently.

In most cases, patients will only experience moderate symptoms and may not receive therapy until the swelling and pain have lasted for an extended period. It is not known for certain what triggers Kohler's sickness. Some orthopedic professionals believe that Kohler's disease may be linked to an injury that occurred in the region surrounding the navicular bone in the foot. They also believe that the condition may be the result of delayed bone ossification. Ossification of the skeleton typically begins between the ages of 18 and 24 months in females and between 24 and 30 months in males (4). There is a possibility that an increase in the ratio of collagen to the bone will lead to structural weakening. Because it is an integral part of the mechanism, such as articulation, that allows the foot to move, the navicular bone is vulnerable to the weight-bearing strains and stresses that are associated with turning and twisting (5).

Under typical conditions, the navicular bone is supplied with blood by a vasculature, which then serves as the origin for smaller arteries that deliver blood to the areas of the growing bone. When a child is between the ages of 4 and 6, additional blood arteries begin to reach parts of the growing bone that require an increased blood supply. If ossification is delayed and the infant experiences weight gain, this can cause the blood vessels to become compressed, which can lead ischemia and then death of tissue (6). Although it has been hypothesized that genetics may play a role in the progression of Kohler's disease, research has not been successful in identifying a particular gene that is connected with this condition. Kohler's disease manifests itself in young males around one year after it has developed in young girls. This is because the Kohler's disease target, the center of bone formation, emerges in young girls. It is estimated that fewer than 2% of the population have the disorder (4).

Epidemiology and etiology

Due to the fact that not all patients suffering from Kohler's disease exhibit symptoms, the prevalence of this condition are not thoroughly established. The prevalence of Kohler's illness among children is approximately 2%. Kohler's illness is observed more frequently in children between the ages of 4 and 7 years old, and it is five times more likely to impact males than it is to affect females (7).

Pressure on the navicular bone before its ossification is assumed to be the root cause of the condition. This results in blood flow irregularities, leading to AVN. In most cases, Kohler's illness affects only one side of the body; however, one study indicated that 25% of cases of Kohler's disease affect both sides of the body (8). Patients will often appear with symptoms, including pain on the medial side of the foot, edema on the medial foot, and/or a limp. On plain radiographs, the navicular will exhibit typical signs of AVN, such as sclerosis, disintegration, and flattening of the bone. This condition is caused by the death of blood vessels. The prognosis is very favorable. There were no examples of Kohler's illness that have developed into long-term clinical or radiographic problems that have been recorded (9).

Histopathology

A bone biopsy is not required to make a diagnosis of Kohler's disease, and it is not suggested for making the diagnosis unless it is necessary to rule out the presence of infection or cancer in the patient. Kohler's disease looks pretty similar to other kinds of AVN histopathologically. Dead cartilages distinguish AVN with empty lacunae that are stained more deeply than healthy bone. This is the predominant histologic hallmark of this condition. The lacunae will become more cystic and have an expanded appearance. It has been discovered that the bone marrow is a more sensitive sign of AVN than the bone body, displaying fat necrosis and calcifications. Patients frequently report concerns regarding dorsomedial midfoot pain when they visit their pediatricians. During the examination, the doctor may find that the patient has point discomfort over the navicular in addition to or instead of redness, heat, and inflammation. If the patient is asked to walk, they may have antalgic limps categorized by walking on the left side of their ankle (10).

When it comes to making a diagnosis of Kohler's disease, plain radiography pictures are the imaging modality of choice. As a result of the bone collapse, the navicular will appear like a wafer. The bone will have a fractured appearance, and the trabecular structure will be absent. Patchy sclerosis of the bones and an enhanced radiodensity are both things that will occur. Soft tissue enlargement can also be observed on computed tomography, which is occurring surrounding the damaged navicular bone. Advanced medical imaging techniques such as CT and MRI are not essential for identification; nevertheless, in the event that the patient's condition does not improve in response to treatment, these techniques may be needed to define diagnosis and follow-up patient. It is essential to connect radiographic observations with clinical

suspicions, even if navicular sclerosis could be consistent with a normal variation in patients presenting. When an infection is suspected, routine laboratory tests must be performed. These tests include a complete blood count, C-reactive protein, and erythrocyte sedimentation rate. If any of the following are elevated, an additional test must be done (11).

Diagnosis

In children, Kohler's disease is frequently misdiagnosed as osteomyelitis. However, standard laboratory tests will be able to assist in distinguishing between the two pathologies. When a child has a high erythrocyte sedimentation rate or C-reactive protein level, there ought to be a high index of suspicion that they have an infection. Inflammatory markers will not be increased in a patient with Kohler's disease, and increased inflammatory indicators should not be present in a pediatric child (12). In the event that it is thought that an infection is present, it may be necessary to do a bone aspiration, a bone biopsy, or blood cultures. The outlook for patients suffering from Kohler's illness is very favorable, and up to this point, there were no reports of any long-term symptoms or disabilities in Kohler's disease patients who were children. Approximately six to forty-eight months after the onset of symptoms, radiographs will begin to show signs of improvement. In the absence of casting, symptoms normally disappear within six to nine months. Patients treated with plaster casts (non-weight bearing) were pain-free after an average of three months. Although arch support orthopedics reduced local discomfort, researchers discovered that the symptoms persisted for an average of seven months (13, 14).

Treatment and management

Patients should be referred to a pediatric orthopedic surgeon for further assessment if there is even a remote possibility that Kohler's disease is present. Kohler's disease is managed with a cautious approach to therapy (15). Non-steroid anti-inflammatory drugs can help reduce the severity of symptoms, but there is no evidence that they can speed up the resolution of illness symptoms. Patients can have their symptoms reduced in duration by having their lower legs restrained in a walking cast for a period of four to six weeks. It is difficult to determine the effect of weight-bearing casting as opposed to non-weight-bearing casting, and the outcome is frequently reliant on the surgeon. There have been some accounts of people utilizing offloading orthotics for symptomatic alleviation; however, it does not appear that orthotics cut down on how long people deal with their symptoms. Therefore, there is no justification for surgery for Kohler's disease. If the patient's symptoms do not begin to improve, the doctor needs to examine other potential diagnoses. In about six months, we should see indications of improvement in both the radiography and the symptoms (13).

The disorder is typically managed with restraint and close monitoring in most instances. No long-term radiological or clinical signs of Kohler's illness are recorded in the medical literature, indicating that individuals with Kohler's disease have an excellent safety profile.

CONCLUSION

Kohler's disease affects children. The pressure of the navicular bone before ossification is suggested to cause it. Blood flow anomalies cause AVN. Kohler's illness affects 4 to 7-year-old boys, and 20% of Kohler's disease cases are bilateral. Medial foot soreness, edema, and limping are common symptoms, and the navicular demonstrates sclerosis, disintegration, and flattening on plain films. Kohler's disease has a good prognosis. There have been no known cases of Kohler's illness generating primary care physician or radiographic problems.

REFERENCES

1. Tsirikos AI, Riddle EC, Kruse R. Bilateral Kohler's Disease in Identical Twins. *Clinical Orthopaedics and Related Research*. 2003;409:195-198. doi:10.1097/01.blo.0000057993.41099.d5
2. Shastri N, Olson L, Fowler M. Kohler's disease. *Western Journal of Emergency Medicine*. 2012;13(1):119-120. doi:10.5811/westjem.2011.1.6691
3. Karr JC. External Fixation Diastasis Management of Kohler's Disease in a 14-Year-Old Boy: A Case Report. *Journal of the American Podiatric Medical Association*. 2020;110(3). doi:10.7547/17-140
4. Khan AQ, Sherwani MA, Gupta K, Siddiqui YS, Hali NZ. Kohler's disease. *Saudi Medical Journal*. 2008;29(9):1357-1358.

5. Bui-Mansfield LT, Lenchik L, Rogers LF, Chew FS, Boles CA, Kline M. Osteochondritis Dissecans of the Tarsal Navicular Bone: Imaging Findings in Four Patients. *Journal of Computer Assisted Tomography*. 2000;24(5):744-747. doi:10.1097/00004728-200009000-00015
6. Devine KM, Van Demark RE. Kohler's osteochondrosis of the tarsal navicular: case report with twenty-eight year follow up. *South Dakota Journal of Medicine*. 1989;42(9):5-6. https://pubmed.ncbi.nlm.nih.gov/2799378/
7. Dobbe AM, Gibbons PJ. Common paediatric conditions of the lower limb. *Journal of Paediatrics and Child Health*. 2017;53(11):1077-1085. doi:10.1111/jpc.13756
8. Weiss JE, Stinson JN. Pediatric Pain Syndromes and Noninflammatory Musculoskeletal Pain. *Pediatric Clinics of North America*. 2018;65(4):801-826. doi:10.1016/j.pcl.2018.04.004
9. de Herder WW. The History of Acromegaly. *Neuroendocrinology*. 2015;103(1):7-17. doi:10.1159/000371808
10. Aktas E. Spontaneous and bilateral avascular necrosis of the navicula: Müller-Weiss disease. *Joint Diseases and Related Surgery*. 2016;27(3):179-182. doi:10.5606/ehc.2016.36
11. Houlden R. Does immobilisation improve outcomes in children with Köhler's disease? *Archives of Disease in Childhood*. 2020;106(3):303-305. doi:10.1136/archdischild-2020-320548
12. Langley CR, Garrett SJ, Urand J, Kohler J, Clarke NM. Primary multifocal osseous Hodgkin's lymphoma. *World Journal of Surgical Oncology*. 2008;6(1). doi:10.1186/1477-7819-6-34
13. Khoury J, Jerushalmi J, Loberant N, Shtarker H, Militianu D, Keidar Z. Kohler Disease: Diagnoses and Assessment by Bone Scintigraphy. *Clinical Nuclear Medicine*. 2007;32(3):179-181. doi:10.1097/01.rlu.0000255026.52044.85
14. Borges JLP, Guille JT, Bowen JR. Köhler's Bone Disease of the Tarsal Navicular. *Journal of Pediatric Orthopaedics*. 1995;15(5):596-598. doi:10.1097/01241398-199509000-00009
15. Santos L, Estanqueiro P, Matos G, Salgado M. Köhler disease: an infrequent or underdiagnosed cause of child's limping? *Acta Reumatologica Portuguesa*. 2015;40(3):304-305.

European Journal of Musculoskeletal Diseases
ISSN 2038-4106/2021

Letter to the Editor

BRITTLE BONE DISEASE

E. Qorri[1,*] and P. Daliu[1]

[1]Dental School, Albanian University, Tirana, Albania

[*]*Correspondence to:*
Erda Qorri, DDS
Dean Dental School, Albanian University, Tirana, Albany
e-mail: e.qorri@albanianuniversity.edu.al

ABSTRACT

Osteogenesis imperfecta (OI), sometimes called brittle bone disease (BBD), is an inherited genetic illness marked by extreme bone fragility or brittleness. Families can pass on the BBD to their offspring. A mutation in the gene that produces collagen causes it. When type I collagen levels are lowered, bones become brittle and more vulnerable to fractures. BBD types II, III, and IV results from mutations in the COL1A1 and COL1A2 genes. Osteoid synthesis is typically inadequate due to abnormalities such as reduced collagen type I production or aberrant collagen secretion. As a result, both intramembranous, as well as enchondral ossification are impacted. The usual histological features are a large, uneven physics with disordered proliferative and hypertrophy zones and a calcified thinning zone. Other features include sparse spongiosa, bone resorption, and accelerated bone turnover. For the development and evaluation of treatment in people with heritable illnesses, a thorough clinical description containing the knowledge of precise molecular genetic aetiology is the starting point. This article aims to cover the histology, diagnosis, and therapy of three types of BBD to make it easier to assess the situation and suggest fresh alternatives to surgery.

KEYWORDS: *Brittle bone disease, Osteogenesis imperfect, clinical manifestation, bone, resorption, fracture*

INTRODUCTION

Brittle bone disease (BBD), also known as osteogenesis imperfecta (OI), is a genetically inherited condition accompanied by high bone brittleness or fragility. BBD is transmitted via families. It is triggered by a mutation in a gene that makes collagen. Bones become brittle and more prone to fractures when type I collagen levels are reduced. BBD types II, III, and IV are caused by mutations in the COL1A1 and COL1A2 genes. These polymorphisms often alter the sequence of type I collagen subunits, leading to aberrant type I collagen. Although a child can inherit this gene from both parents, most infants with BBD only inherit it from one. The genetic variant can occasionally arise as a fresh mutation (1). Clinical characteristics are typically used to distinguish between four main categories. Patients with type I have a

Received: 18 October 2020
Accepted: 13 January 2021

ISSN: 2038-4106

moderate presentation and frequently are of higher average age, while type II is typically fatal during the prenatal period. In children who survive the newborn period, Type III is by far the most severe kind. These individuals have an identifiable phenotype that includes multiple fractures, short height, anomalies of the growth plate, and developing limb and spinal deformities. Type IV patients are those with mild to severe phenotypic who do not fall into one of the abovementioned groups. It is evident that this is a diverse set of illnesses, and some type IV patients exhibit characteristics that contradict the Sillence categorisation (2). A hyperplastic callus is one of these characteristics, and it can develop following fractures or reconstructive surgery. Hyperplastic callus usually manifests as a warm, severe, and firm swelling over the damaged bone, which may imply a differential diagnosis with sarcoma and inflammation. Excessive formation of poorly structured, partially calcified extracellular matrix is visible at the microscopic level. The shape and size of the callouses may stay constant for several years after a phase of fast growth (3).

Other symptoms include dentinogenesis imperfecta, blue sclerae, small height, and adult deafness. Aortic root enlargement and valvular insufficiencies have also been reported. Some milder signs are generalised flexibility, easy bleeding, hernias, and excessive sweating. Clinical signs range from moderate, completely asymptomatic type to most severe variants, which involve infants arriving with crumpled bones, a fragile skull, and lengthy bone fractures inconsistent with life, leading to neonatal mortality (4).

Epidemiology

BBD is thought to occur in about 1 out of every 20,000 births. BBD is thought to be prevalent across the United States at a rate of 20,000–50,000 people; this makes it an orphaned disease, that is, one that only affects 200,000 people or less in the United States (5). According to reports, there are 2.35 to 4.7 cases of type I OI per 100,000 people worldwide. Type II OI is reported to occur between 1 in 40,000 and 1.4 in every 100,000 live births. Even though the prevalence is significantly less frequent than type I, the precise incidence of kinds III and IV OI is unknown. Congenital A (19%), congenital B (31%), tarda A (25%) and tarda B incidence rates were roughly 25% in Shapiro's study (6).

Pathophysiology

A quantitative reduction in the number of structural, normal type I collagen can be brought on by frameshift mutations (which involve a premature termination codon in the afflicted allele). Heterozygous for this syndrome, a patient may produce half as much type I collagen as is typical. PLS3/ AD, COL1A1 and COL1A2 / X-linked mutations are involved. As an alternative, alteration in the form of substitutions or deletion in the polypeptide chain containing a glycine peptide sequence might lead to the formation of collagen that is structurally or quantitatively aberrant or less effective. Whether glycine is substituted at the carboxy-terminal (extreme condition) or amino-terminal (mild version) of the protein molecules determines the phenotypic variation of these abnormalities (7).

Due to the triple helix's starting to cross-link at the carboxy terminus of polypeptide chains, mutations at the carboxy end of the peptide may be more harmful. These patients experience more severe skeletal symptoms than those who have haploinsufficiency abnormalities. Mutations cause haploinsufficiency abnormalities at glycine sites that alter the integrity of collagen strands, a defect frequently found in types II, III, and IV (7). Type II (perinatal) Mutations are COL1A2, AD, CRTAP, AR / COL1A1, PPIB, LEPRE1, and BMP1. In type III (progressively deforming) are AD, COL1A2, AR / COL1A1, CRTAP, PPIB, LEPRE1, FKBP10, SERINF1, SERPINH1, and WNT1. In type IV (moderate) are AD, COL1A2, CRTAP, AR / COL1A1, SP7, FKBP10, WNT1, SERPINF1, and TMEM38B. Calcification of interosseous membrane or hypertrophic callus-type V has mutations found in AD / IFITM5 (8, 9).

Diagnosis

A relatively low stature does not rule out the diagnoses in type I OI because patients frequently have normal statures. Type I OI is not the same as mild OI. People may experience a few or no fractures, typically in the first few years of their lives, or many fractures throughout their lifetimes. Their faces could be triangular. They have complete mobility and no lengthy bone bowing, yet they could have osteoporotic fractures. Most people have blue sclera, although it can also be white or lose its blue tint with age. It is an autosomal dominant feature passed down from parent to child (10).

The apparent lack of relevance of bone density in individuals with OI is highlighted by the fact that bone density can be extremely low even in the lack of fractures and has no link to clinical severity.
In many cases, bone density is typical during the first few months of birth, and their ability to enhance bone mineral density declines as they age. Sometimes the diagnosis is a chance discovery following a fracture. Even in very mild cases, dentinogenesis imperfecta may exist. These people may have early hyperacusis, cardiac problems, and aortic valvular diseases (11, 12).

Patients with type IV are often diagnosed based on their small stature, lengthy bone bending, and spinal fractures. In addition, there could be joint slackness and scoliosis. Patients with this type of OI can typically ambulate; however, they might need assistance when walking. The sclera in these patients is white. Because the clinical symptoms of this kind of OI are not well described in the literature and because different centres use different diagnostic standards, accurate identification is frequently challenging (13). Due to their larger heads and underdeveloped facial bones, these individuals have triangle faces. They also have significant long bone malformations, vertebral injuries, chest abnormalities, and scoliosis. They are also noticeably low in stature. Despite some of them being capable of walking with assistance, they typically use a wheelchair. Ultrasonography can occasionally be used to make difficult prenatal testing. A "popcorn look" is a unique structural modification of the metaphyses and epiphyses of long bones caused by altered growth circular plates. Respiratory problems in severe cases may make survival riskier (14).

Most infants with this type of OI do not survive the prenatal period. The central nervous system's abnormalities or haemorrhages, the ribs' severe brittleness, or pulmonary hypoplasia are all potential causes of death. In addition, the infants have numerous intra-uterine fractures, including injuries to the skull, bony protrusions and vertebra, beaded sternum, and significant long bone deformity. It is typically impossible to differentiate between severe and deadly OI during pregnancy. In really severe circumstances, birth might result in dismemberment. Most cases include autosomal dominant novel mutations. It has been hypothesised that deadly OI may come in various clinical presentations. Despite the severity, some individuals have endured it for a long time (15).

Histopathology

Lamellar on woven bone synthesis is demonstrated as a compel self-assembly system and bone synthesis having followed the normal developmental pattern, but showing factor delay in growth and development caused by missense mutation or insufficient quantities of the collagen matrix, according to explanation in the context of woven to membranous bone growth by mesenchymal and surface osteoblasts, respectively (16). The more extreme the BBD variety, the more persistent the woven bone is and the more immature the morphological pattern is. Once a minimum accumulation for an acceptable framework of woven bone has been achieved, the pattern changes to a structurally firmer lamellar configuration. Lethal perinatal variants are characterised by woven bone alone; gradually deforming variants have varying quantities of woven plus lamellar bone, and lamellar bone progressively develops rudimentary, then partially compressed osteons without achieving full compaction. Lamellar bone is characterised by short, vertically oriented laminae with a mosaic pattern in increasingly deforming forms at various levels of microscopic magnification; polarisation specifies tissue conformational changes and localises lamellar formation beginning. Ultrastructure of bone-forming cells reveals significantly dilated rough endoplasmic reticulum, notable Golgi bodies, disoriented cisternae, swollen scattered tubules and vacuoles, structural indicators of storage disorder/stress responses, and mitochondrial inflammation in cells with significantly dilated rough endoplasmic reticulum indicating cell death (17).

Treatment

After a thorough evaluation by the treating physician, many children with OI start receiving bisphosphonate (BP) medication to reduce osteoclast activity. In this sense, cyclical intravenous BP treatment has emerged as the preferred method for treating children with moderate to severe OI. A relatively recent randomised, placebo-controlled double-blind trial of oral Risedronate in children with OI, which included many children who were more mildly to moderately affected, revealed a significant reduction in fracture risk, expanding the beneficial properties of this medication in children with OI (18). Unfortunately, by the conclusion of the early decades in the past, about two-thirds of patients had passed away. Kyphoscoliosis, pulmonary oedema, and cardio-respiratory insufficiency were the sequelae of skeleton chest wall deformities that typically led to death. It is believed that most patients with OI type III will live into adulthood, given the

current therapeutic choices, particularly BP treatment with cyclic injectable pamidronate started in infancy (19). Studies show that centres of competence treating children with severe OI achieve very low fracture incidence and close to normal development rates in newborns who started receiving cyclic injectable pamidronate by the age of three. The treatment seems to be well accepted, and studies have shown that it raises bone density, lowers the frequency of fractures, and improves vertebral form (20, 21).

The effectiveness of BPs (oral or intravenous) administration on patients affected by BBD is still debatable. A systematic review reported conflicting results since Dwan et al. (22) concluded that studies included in their analysis do not show BPs conclusively improve clinical status (reduce pain; improve growth and functional mobility) in people with OI, whereas Ying et al. (23) reported significant improvement of bone mineral density in patients affected with OI when treated with oral BPs. Finally, Constantino et al. (24) showed that randomised controlled trials did not demonstrate a significant improvement in function and mobility with oral BPs administration. In contrast, non-randomised open-label uncontrolled studies demonstrated that oral and intravenous BPs administration objectively improved function and mobility.

Phenotyping is of paramount importance for diagnosing, classifying, and evaluating OI severity, giving patients and associated families knowledge about the likely progression of the condition and enable doctors to assess the effectiveness of therapy. For developing and evaluating treatment in people with heritable illnesses like OI, a thorough clinical description knowledge and understanding of the precise molecular genetic aetiology is the starting point (25).

CONCLUSION

Although there have been suggestions that there could be different types of OI, the most common description of BBD separates the condition into four categories. These types have names that are numerical, eponymous, or descriptive. Some diseases can be regarded as congenital varieties of OI-like brittle bones. For developing and evaluating treatment in people with heritable illnesses like OI, a thorough clinical description containing the knowledge of precise molecular genetic aetiology is the starting point.

REFERENCES

1. Glorieux FH, Rauch F, Plotkin H, et al. Type V osteogenesis imperfecta: a new form of brittle bone disease. *Journal of Bone and Mineral Research: The Official Journal of the American Society for Bone and Mineral Research*. 2000;15(9):1650-1658. doi:10.1359/jbmr.2000.15.9.1650
2. van Dijk FS, Cobben JM, Maugeri A, Nikkels PGJ, van Rijn RR, Pals G. [Osteogenesis imperfecta: clinical and genetic heterogeneity]. *Nederlands Tijdschrift Voor Geneeskunde*. 2012;156(21):A4585.
3. Vieira RLV, Amaral DT, Jesus-Garcia FR, Saraiva G, Fernandes ARC, Resnick D. Hyperplastic callus formation in osteogenesis imperfecta type V mimicking osteosarcoma: 4-year follow-up with resolution. *Skeletal Radiology*. 2006;35(6):402-405. doi:10.1007/s00256-005-0039-3
4. Forlino A, Cabral WA, Barnes AM, Marini JC. New perspectives on osteogenesis imperfecta. *Nature Reviews Endocrinology*. 2011;7(9):540-557. doi:10.1038/nrendo.2011.81
5. Marini JC. Osteogenesis imperfecta: comprehensive management. *Advances in Pediatrics*. 1988;35:391-426.
6. Shapiro F. Consequences of an Osteogenesis Imperfecta Diagnosis for Survival and Ambulation. *Journal of Pediatric Orthopaedics*. 1985;5(4):456-462. doi:10.1097/01241398-198507000-00014
7. Makareeva E, Mertz EL, Kuznetsova NV, et al. Structural heterogeneity of type I collagen triple helix and its role in osteogenesis imperfecta. *The Journal of Biological Chemistry*. 2008;283(8):4787-4798. doi:10.1074/jbc.M705773200
8. Rauch F, Lalic L, Roughley P, Glorieux FH. Relationship Between Genotype and Skeletal Phenotype in Children and Adolescents With Osteogenesis Imperfecta. *Journal of Bone and Mineral Research*. 2010;25(6):1367-1374. doi:10.1359/jbmr.091109
9. Rossi V, Lee B, Marom R. Osteogenesis imperfecta - advancements in genetics and treatment. *Current opinion in pediatrics*.

2019;31(6):708-715. doi:10.1097/MOP.0000000000000813
10. Smith R. Osteogenesis imperfecta. *Clinics in Rheumatic Diseases*. 1986;12(3):655-689.
11. Shapiro JR, Pikus A, Weiss G, Rowe DW. Hearing and middle ear function in osteogenesis imperfecta. *JAMA*. 1982;247(15):2120-2126.
12. Plotkin H. Syndromes with congenital brittle bones. *BMC Pediatrics*. 2004;4(1). doi:10.1186/1471-2431-4-16
13. Brizola E, Staub ALP, Félix TM. Muscle Strength, Joint Range of Motion, and Gait in Children and Adolescents With Osteogenesis Imperfecta. *Pediatric Physical Therapy*. 2014;26(2):245-252. doi:10.1097/pep.0000000000000042
14. Van Dijk FS, Sillence DO. Osteogenesis imperfecta: clinical diagnosis, nomenclature and severity assessment. *American journal of medical genetics Part A*. 2014;164A(6):1470-1481. doi:10.1002/ajmg.a.36545
15. Sinikumpu JJ, Ojaniemi M, Lehenkari P, Serlo W. Severe osteogenesis imperfecta Type-III and its challenging treatment in newborn and preschool children. A systematic review. *Injury*. 2015;46(8):1440-1446. doi:10.1016/j.injury.2015.04.021
16. Hoyer-Kuhn H, Netzer C, Semler O. Osteogenesis imperfecta: pathophysiology and treatment. *Wiener Medizinische Wochenschrift*. 2015;165(13-14):278-284. doi:10.1007/s10354-015-0361-x
17. Mendelson KL. Critical review of "temporary brittle bone disease." *Pediatric Radiology*. 2005;35(10):1036-1040. doi:10.1007/s00247-005-1573-9
18. Bishop N, Adami S, Ahmed SF, et al. Risedronate in children with osteogenesis imperfecta: a randomised, double-blind, placebo-controlled trial. *The Lancet*. 2013;382(9902):1424-1432. doi:10.1016/s0140-6736(13)61091-0
19. Alcausin MB, Briody J, Pacey V, et al. Intravenous pamidronate treatment in children with moderate-to-severe osteogenesis imperfecta started under three years of age. *Hormone Research in Paediatrics*. 2013;79(6):333-340. doi:10.1159/000351374
20. DiMeglio LA, Ford L, McClintock C, Peacock M. Intravenous pamidronate treatment of children under 36 months of age with osteogenesis imperfecta. *Bone*. 2004;35(5):1038-1045. doi:10.1016/j.bone.2004.07.003
21. Munns CF, Rauch F, Travers R, Glorieux FH. Effects of Intravenous Pamidronate Treatment in Infants With Osteogenesis Imperfecta: Clinical and Histomorphometric Outcome. *Journal of Bone and Mineral Research*. 2005;20(7):1235-1243. doi:10.1359/jbmr.050213
22. Dwan K, Phillipi CA, Steiner RD, Basel D. Bisphosphonate therapy for osteogenesis imperfecta. *Cochrane Database of Systematic Reviews*. 2016;10(10):CD005088. doi:10.1002/14651858.cd005088.pub4
23. Ying ZM, Hu B, Yan SG. Oral Bisphosphonate Therapy for Osteogenesis Imperfecta: A Systematic Review and Meta-Analysis of Six Randomised Placebo-Controlled Trials. *Orthopaedic Surgery*. 2020;12(4):1293-1303. doi:10.1111/os.12611
24. Constantino CS, Krzak JJ, Fial AV, et al. Effect of Bisphosphonates on Function and Mobility Among Children With Osteogenesis Imperfecta: A Systematic Review. *JBMR Plus*. 2019;3(10):e10216. doi:10.1002/jbm4.10216
25. Biggin A, Munns CF. Osteogenesis Imperfecta: Diagnosis and Treatment. *Current Osteoporosis Reports*. 2014;12(3):279-288. doi:10.1007/s11914-014-0225-0

European Journal of Musculoskeletal Diseases
ISSN 2038-4106/2021

Letter to the Editor

KIENBÖCK'S DISEASE

V. Sollazzo

Medical Director, Medical Center, Ferrara, Italy

Correspondence to:
Vincenzo Sollazzo, MD
Orthopedic Surgeon, Medical Director, Medical Center, Ferrara, Italy
e-mail: slv@unife.it

ABSTRACT

Persistent avascular osteonecrosis of lunate bone is the medical term for the uncommon condition known as Kienböck's disease (KD). The typical indications of this condition include a restriction in motion on one side of the wrist and pain and oedema in that area. Although there have been some recent developments in therapeutic approaches, the etiology and pathophysiology of the condition are still not well understood. In addition to direct trauma, frequent risk factors include anatomical traits such as ulnar variation, changes in blood flow, and more significant intraosseous pressure. Radiographic features evaluated using a modified version of the Lichtman scale are the primary factor in determining the KD stage. The selection of treatment choices is frequently challenging because radiographic findings do not always precisely match the first clinical symptoms and can vary depending on the patient's age group. When KD is detected in its initial stages, nonoperative therapy consisting of unloading is typically recommended. Vascularized bone grafting is one of the most recent surgical methods implemented in Stage III cases. A vascularized, pedicled scaphoid graft combined with partial radioscaphoid arthrodesis is one of the techniques that have been reported. This approach provides good pain control and prevents carpal collapse.

KEYWORDS: *Kienböck's disease, lunatomalacia, lunate, carpal bone, ulnar bone*

INTRODUCTION

Avascular degeneration of the lunate carpal bone, also known as lunatomalacia, is referred to as Kienböck's disease (KD). Austrian physician Robert Kienböck initially identified and characterized it in 1910 (1). This disease's origin is still a mystery, and there is some debate on what caused it. On the other hand, it is feasible to identify elements that, in general, have an impact on the probability of incidence. The coverage of the lunate by the radius, the blood flow, excessive intracoronary pressure, and venous stasis are all anatomic risk factors. Other anatomical risk factors include the form of the lunate and proximal radial distance, ulnar variation, and the protection of the lunate by the radius. Currently, there is no evidence to suggest the existence of medication with the potential to regress the disease or even arrest the advancement (2). The fact that there are many other names for KD, such as lunate malacia, idiopathic, aseptic, avascular, or acute lunate

Received: 29 October 2020
Accepted: 2 aprile 2021

ISSN: 2038-4106

necrosis, suggests that the actual cause of the condition is still not well recognized. In addition, there is a lack of clarity on diagnostic criteria, which contributes to the unknown frequency and prevalence of the condition.

The undetermined aetiology also contributes to this lack of clarity. On the other hand, KD is a disease with a prevalence of fewer than 5 in every 10,000 individuals (3). Personal factors consist of age and ethnicity, as well as trauma-related variables, environmental factors, and the association with osteonecrosis of all other carpal bones (4). Other related disorders include osteoarthritis. The incidence of KD is approximately 7 in every 100,000 people (5, 6), which places it in the category of a rare condition. Males are more likely to be affected by KD, and the age range of 20–40 years has the highest incidence (7). In the past, manual labor was thought to be a risk factor, but it is more that it exacerbates symptoms of an illness already diagnosed (8).

In most cases, only one hand is affected; only 4% of people have the condition on both hands. It is well established that KD is linked to a higher risk of developing systemic lupus erythematosus, type 1 diabetes mellitus, and Legg-Calve-Perthes disease (7). During the examination, it was found that there was a severe swelling on the dorsal surface of the lunate. Typical symptoms include a reduced range of motion in the wrist as well as reduced grip strength (9).

Anatomy

Compared to the distal carpal row, which is more or less immobile, the proximal array of carpal bones in the midcarpal joint is primarily responsible for the movement of the wrists. The lunate is the bone that is located in the middle of the proximal array. It articulates with the scaphoid, triquetrum, capitate, and sometimes the hamate. The lunate is a component of the radiocarpal joints and articulates via the triangle fibrocartilage complex with the ulna. More anteriorly, the lunate is located on the palm side of the forearm. Noteworthy is the fact that approximately 10% of the axial-radial/ulnar/carpal load is transmitted through the triangle fibrocartilage complex and, in turn, to the ulna, whereas 35% of the force is delivered through radio-lunate articulation (10, 11).

Epidemiology and aetiology

Avascular degeneration of the scaphoid is the most frequent type of avascular necrosis of the carpal bones. KD is the second most prevalent type of avascular necrosis of the bones. The population that is typically affected consists of guys between the ages of 20 and 40 (12). There is still no widespread agreement regarding the most important contributor to the development of KD. It can be attributed to a number of factors. The term “ulnar negative variance” (sometimes written as “ulna minus”) describes a situation in which the ulna is abnormally shorter in comparison to the radius. Because of the comparatively long radius, the lunate suffers from excessive mechanical stress and recurrent microtrauma when the ulna is too short.

According to several kinds of research, this finding is correlated with 78% or more of the instances of KD (13). The lunate bone receives its vascular supply from various dorsal and volar penetration arteries that branch off the dorsal and palmar radiocarpal and intercarpal arches. These arteries penetrate the dorsum of the lunate. There aren’t many intraosseous collaterals (12, 14).

Given the structure of the lunate, the chances of developing KD rise when the size of the lunate diminishes, as this causes the lunate to bear a greater axial load. The lunate can have the shape of a square or rectangle, or it may have the shape of a triangle, in which case the medial articular facet will not be present (type I, see below). This latter condition, a risk factor for the emergence and advancement of the disease, is distinguished by a more fragile trabecular pattern (15). The radial angle of inclination determines the angle produced between the baseline and a line drawn from the ulnar point of the superficial radial layer to the tip of the radial styloid. This line begins at the superficial radial layer and ends at the radial styloid. As the horizontal inclination angle becomes more shallow, the likelihood of getting KD becomes more severe (16).

Evaluation

Patients typically appear with unilateral pain across the dorsal area of the wrist, limited wrist motion, stiffness, or a combination of all three of these symptoms at the time of their initial evaluation. The pain is made worse by extending the wrist and axial stress. The severity of the symptoms might range from mild to incapacitating. Rarely does it affect both sides, and trauma is usually not present. During a physical examination, it is typical to find that the patient’s wrist has swollen, that there is discomfort over the predicted placement of the lunate, that they have synovitis, and that they have lost grip strength (17).

KD can be diagnosed based on clinical symptoms and imaging results. Radiography/computed radiography and MRI are two techniques with a high degree of diagnostic accuracy. Nevertheless, MRI has the highest level of sensitivity

and can identify radiographically occult instances. The disease is characterized by a diffuse decrease in the lunate bone marrow signal, which can be seen using MRI. The progression and severity of osteonecrosis both cause different kinds of signal alterations. In addition, the integrity of the articular cartilage can be evaluated using MRI (7).

Early on in the disease, the radiographs were normal. Observations, when present, depend on the morphology stage and include diffused lunate degeneration, cystic alterations, articular surfaces collapse, wrist collapse, and mid/radio-carpal secondary arthrosis, among other things. Lunates with a type I morphological structure (see below) are susceptible to developing coronal fractures (17). Therefore, the use of computerized tomography in surgical planning can be beneficial. In addition, it is more sensitive than radiographs when detecting small subchondral fractures, coronal lunate fractures, fragments, carpal instability, and the degree to which trabecular disruption has occurred. After CT imaging, several affected patients changed their stages (18).

Staging

Examining radiographic images is mainly used to stage KD (19). However, clinical relevance also extends to examining cartilage and vasculature (20). Accurate disease categorization is crucial when deciding on the best course of treatment for a patient with osteonecrosis of the lunate. The lunate maintains typical architecture and thickness in stage I, producing typical plain radiographs (9). After contrast has been applied, the lunate is frequently substantially increased at this point, reflecting marrow edema. Radiographs taken at Stage II reveal increased lunate density and widespread sclerosis, but the architecture of the wrist is unaffected. Stage III is when the lunate passes out. Stage III was initially separated into stages 3A and 3B in 1993, while stage 3C was later added in 2010 (6). The lunate is compressed in stage IIIA, but its carpal position and height are unaltered. A cortical "ring sign" on radiographs indicates that stage IIIB is characterized by articular collapse, the distal migration of the capitate, and scaphoid palmar flexion (21). No matter how the lunate or wrist morphology is arranged, stage IIIC is only allocated for a complete coronal plane split. Lunate collapses and radio/midcarpal degenerative arthritis make up stage IV (7).

Management and treatment

The treatment for KD aims to alleviate discomfort while preserving the wrist's range of motion and the patient's ability to maintain a firm grasp. The treatment for KD is determined by the disease's stage and the circumstances that cause it. Restriction in a splint or cast is the standard treatment for stage I injuries. Immobilization is another treatment option for stage II, provided the necrosis has not yet reached its final stage. An operation known as "joint-levelling" is required for stages II with total necrosis, III, and IV. This surgery may be combined with vascular implants or the transfer of branches from nearby arteries. In later phases, when there is lunate collapsing and secondary wrist degenerate arthrosis, proximal row corpectomy and intercarpal arthrodesis may also be required. In cases with coexisting ulnar negative variance, the radial shortening osteotomy is the treatment that is performed the most frequently to unload the lunate. In the later stages of the disease, treatment may help relieve symptoms and performance without affecting imaging results (13, 17, 18).

CONCLUSION

The best treatment for Kienböck's is still debatable. Hand surgeons must choose the best treatment strategy; clinical manifestations, radiographic examination, and surgeon expertise should drive the algorithm. Proper disease classification is key to determining the right treatment for osteonecrosis of the lunate. Physical and personal considerations should also be considered.

REFERENCES

1. Wagner JP, Chung KC. A Historical Report on Robert Kienböck (1871–1953) and Kienböck's Disease. *The Journal of Hand Surgery*. 2005;30(6):1117-1121. doi:10.1016/j.jhsa.2005.08.002
2. Fontaine C. Kienböck's disease. *Chirurgie de la Main*. 2015;34(1):4-17. doi:10.1016/j.main.2014.10.149
3. Stahl S, Stahl AS, Meisner C, Rahmanian-Schwarz A, Schaller HE, Lotter O. A systematic review of the etiopathogenesis of Kienböck's disease and a critical appraisal of its recognition as an occupational disease related to hand-arm vibration. *BMC Musculoskeletal Disorders*. 2012;13(1). doi:10.1186/1471-2474-13-225
4. Arora R, Lutz M, Deml C, Krappinger D, Zimmermann R, Gabl M. Long-Term Subjective and Radiological Outcome After

Reconstruction of Kienböck's Disease Stage 3 Treated by a Free Vascularized Iliac Bone Graft. *The Journal of Hand Surgery*. 2008;33(2):175-181. doi:10.1016/j.jhsa.2007.11.005

5. Facca S, Gondrand I, Naito K, Lequint T, Nonnenmacher J, Liverneaux P. Graner's procedure in Kienböck disease: a series of four cases with 25years of follow-up. *Chirurgie De La Main*. 2013;32(5):305-309. doi:10.1016/j.main.2013.07.010
6. van Leeuwen WF, Janssen SJ, ter Meulen DP, Ring D. What Is the Radiographic Prevalence of Incidental Kienböck Disease? *Clinical Orthopaedics & Related Research*. 2016;474(3):808-813. doi:10.1007/s11999-015-4541-1
7. White C, Benhaim P, Plotkin B. Treatments for Kienböck disease: what the radiologist needs to know. *Skeletal Radiology*. 2016;45(4):531-540. doi:10.1007/s00256-016-2332-8
8. Lluch A, Garcia-Elias M. Etiology of Kienböck Disease. *Techniques in Hand & Upper Extremity Surgery*. 2011;15(1):33-37. doi:10.1097/bth.0b013e3182107329
9. Koh S, Nakamura R, Horii E, Nakao E, Inagaki H, Yajima H. Surgical outcome of radial osteotomy for Kienböck's disease—minimum 10 years of follow-up. *The Journal of Hand Surgery*. 2003;28(6):910-916. doi:10.1016/s0363- 5023(03)00490-8
10. Viegas SF, Patterson RM, Todd PD, McCarty P. Load mechanics of the midcarpal joint. *The Journal of Hand Surgery*. 1993;18(1):14-18. doi:10.1016/0363-5023(93)90238-x
11. Schuind F, Cooney WP, Linscheid RL, An KN, Chao EYS. Force and pressure transmission through the normal wrist. A theoretical two-dimensional study in the posteroanterior plane. *Journal of Biomechanics*. 1995;28(5):587-601. doi:10.1016/0021-9290(94)00093-j
12. Murphey MD, Foreman KL, Klassen-Fischer MK, Fox MG, Chung EM, Kransdorf MJ. From the Radiologic Pathology Archives Imaging of Osteonecrosis: Radiologic-Pathologic Correlation. *RadioGraphics*. 2014;34(4):1003-1028. doi:10.1148/rg.344140019
13. van Leeuwen WF, Oflazoglu K, Menendez ME, Ring D. Negative Ulnar Variance and Kienböck Disease. *The Journal of Hand Surgery*. 2016;41(2):214-218. doi:10.1016/j.jhsa.2015.10.014
14. Nealey EM, Petscavage-Thomas JM, Chew FS, Allan CH, Ha AS. Radiologic Guide to Surgical Treatment of Kienbock's Disease. *Current Problems in Diagnostic Radiology*. 2018;47(2):103-109. doi:10.1067/j.cpradiol.2017.04.012
15. Rhee PC, Moran SL. The Effect of Lunate Morphology in Carpal Disorders: Review of the Literature. *Current Rheumatology Reviews*. 2020;16(3):184-188. doi:10.2174/1573397115666190318154322
16. Thienpont E, Mulier T, Rega F, De Smet L. Radiographic analysis of anatomical risk factors for Kienböck's disease. *Acta Orthopaedica Belgica*. 2004;70(5):406-409.
17. Lutsky K, Beredjiklian PK. Kienböck Disease. *Journal of Hand Surgery*. 2012;37(9):1942-1952. doi:10.1016/j.jhsa.2012.06.029
18. Quenzer DE, Linscheid RL, Vidal MA, Dobyns JH, Beckenbaugh RD, Cooney WP. Trispiral tomographic staging of Kienböck's disease. *The Journal of Hand Surgery*. 1997;22(3):396-403. doi:10.1016/s0363-5023(97)80004-4
19. Beredjiklian PK. Kienböck's Disease. *The Journal of Hand Surgery*. 2009;34(1):167-175 doi: 10.1016/j.jhsa.2008.10.012
20. Bain GI, Durrant A. An Articular-based Approach to Kienbock Avascular Necrosis of the Lunate. *Techniques in Hand & Upper Extremity Surgery*. 2011;15(1):41-47. doi:10.1097/bth.0b013e31820e82e8
21. Kennedy C, Abrams R. In Brief: The Lichtman Classification for Kienböck Disease. *Clinical Orthopaedics & Related Research*. 2018;477(6):1516-1520. doi:10.1097/corr.0000000000000595.